基于Mindlin板理论的石英晶体谐振器高频振动分析



王骥 教授
宁波大学压电器件技术实验室
http://piezo.nbu.edu.cn
wangji@nbu.edu.cn

2012压电声波器件分析理论与方法暑期讲习班
2012年8月6-9日·宁波大学

提纲

1. 石英晶体谐振器的历史和趋势
2. 弹性波基础
3. 石英晶体
4. 无限大板的厚度振动
5. Mindlin板方程
6. 复杂因素

提纲

1. 石英晶体谐振器的历史和趋势
2. 弹性波基础
3. 石英晶体
4. 无限大板的厚度振动
5. Mindlin板方程
6. 复杂因素

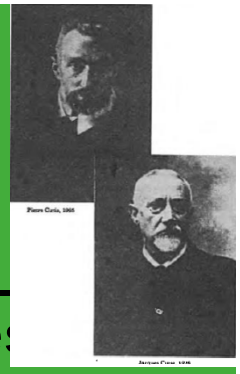
Snapshot of Worldwide Quartz Crystal Resonator Market

- Quartz crystal components market will be about 7 billion USD with a growth rate of 7.5% annually. Year 2009 market is about 6 billion.
- There are about 450 companies and suppliers globally.
- 30% of piezoelectric devices are in telecommunications, while the remaining 70% are in consumer electronics products.
- Japan is supplying the high-end products, while China is producing components for the consumer markets with a global market share about 25%.

Leading Producers of Quartz Crystal Resonators

1. **EPSON-TOYOCM**
2. **NDK**
3. **KYOCERA KINSEKI**
4. **KDS**
5. **VECTRON**
6. **TXC**
7. **TEW**
8. **RAKON**
9. **RIVER**
10. **PERICOM (Taiwan)**
11. **Siward (Taiwan)**
12. **HELE (Taiwan)**
13. **Jingyuan Yufeng (China)**
14. **Taitien (Taiwan)**
15. **Aker (Taiwan)**
16. **TAI-SAW (Taiwan)**
17. **ECEC (China)**
18. **Hubei Dongguang Group (China)**
19. **Nanjing HuaLianXing (China)**
20. **Taizhou Abel Electronics (China)**

Piezoelectricity



- The discovery of Piezoelectricity by the Pierre and Jacques Curie brothers in 1880 is the start of the piezoelectric devices and applications. The direct piezoelectric effect was observed in 1880 and the converse effect in 1881.
- After the Curies the first application of the piezoelectric effect was made by Prof. P. Langevin in France in 1917. Langevin used X-cut plates of quartz to generate and detect sound waves in water.

http://www.ieee-uffc.org/frequency_control/teaching/vig/vig3.htm

http://www.ieee-uffc.org/main/history.asp?file=bottom

http://en.wikipedia.org/wiki/Piezoelectricity

W. P. Mason, Piezoelectricity, its history and applications, *J. Acoust. Soc. Am.* **70** (6), 1561-1566, 1981.

Piezoelectricity-continued

- In 1919, Cady used a quartz piezoid to control the frequency of an oscillator and in a series of papers during the next three years he described the use of quartz bars and plates as frequency standards and wave filters. It is generally accepted that Cady was the first to use a quartz piezoid to control the frequency of an oscillator circuit.
- It remained for Prof. G. W. Pierce of Harvard University to show, in 1923, that a quartz plate with only one set of electrodes could be made to control the frequency of an oscillator circuit using only one vacuum tube. Pierce's circuit has probably been used more than any other quartz crystal oscillator circuit.

Piezoelectricity-continued

- Prof. K. S. van Dyke, a student and colleague of Cady, showed in 1925 that the two electrode piezoelectric resonator is the electrical equivalent of a series resonant circuit shunted by a capacitor.
- In 1923 the *Bell Telephone Laboratories* established a *quartz laboratory* and the *General Electric Company* did likewise the following year. One of the individuals who recognized the potential of the quartz crystal unit was August E. Miller.

Piezoelectricity-continued

- In 1923 Miller left the optical business where he had become an expert in grinding quartz lenses to go into the business of making quartz crystal blanks for amateur radio operators or "hams". ***It appears that Miller may have been one of the first individuals to go into the business of making quartz crystal units***.
- In 1926 the A. T. & T. radio station WEAF (no longer in use) in New York City became the ***first radio station in the United States*** to control its frequency with a quartz crystal unit. Within a few years all radio stations went to crystal control thus providing another small market for quartz crystal units.

Piezoelectricity-continued

- Efforts to develop a practical unit having a low frequency-temperature coefficient were successful in ***1934 when the AT- and BT-cuts*** were discovered independently by ***Koga*** in Japan, by ***Bechmann and Straubel*** in Germany and by ***Lack, Willard,*** and ***Fair*** in the United States.
- Two years later Baldwin and Bokovoy of RCA introduced the V-cut.

Piezoelectricity-continued

- The 1939 decision of the ***Armed Services of the United States to convert its radio equipment to crystal control*** resulted in the creation of an industry which ultimately played an important role in the victory of the Allied Forces over the Axis Powers.
- If any date can be ascribed to the beginning of the quartz crystal industry in the United States it is probably late October or early November 1941 when the Quartz Crystal Section (QCS) was organized in the Office of the Chief Signal Officer (OCSIGO).

Piezoelectricity-continued

- By ***1943 about 130 manufacturers*** were engaged in the production of crystal units. Twenty three of these were in the ***Chicago*** area, 20 in the ***New York*** area, 15 in the ***Carlisle*** area and 14 in the ***Kansas City*** area. The remainder were scattered over 20 states from Oregon to Florida and California to Massachusetts.
- The supervision of so many small plants, distributed over such an area was a major problem and the members of the staff of the QCS spent much time on travel duty instructing the new manufacturers, helping them with technical problems, correlating test equipment and settling arguments between them and the Signal Corps Inspectors.

Piezoelectricity-continued

- The field of piezoelectricity has always been, and continues to be ignored by the Schools of Electrical Engineering. Quartz crystal technology has been treated as an art, or even worse, as ***black magic***.
- With the exception of the students who have received formal training at ***Northern Illinois University*** under Dr. W. E. Newell and at Colorado State University and McMurry College under Dr. Virgil E. Bottom, most of the people in the industry have learned from one another going back to the handful of men who started the industry who had, themselves, learned in the School of Experience.

Piezoelectricity-continued

- Academic neglect of the field is also shown by the dearth of literature available to the newcomer.
- The classic work of Cady (*Piezoelectricity: an introduction to the theory and applications of electromechancial phenomena in crystals*, McGraw-Hill, 1946), the books of W. P. Mason (*Piezoelectric crystals and their application to ultrasonics*, D. Van Nostrand, 1950) and the compilation of 1942 papers by Heising (*Quartz Crystals for Electrical Circuits: Their Design and Manufacture*, D. Van Nostrand, 1946) include practically everything which has been published in this country.
- The book publishers naturally have been reluctant to make the necessary expenditures to publish books for a nonexistent clientele.
- ***Studies on the high frequency vibrations of quartz crystal plates by Koga, Ekstein, and a few others were not well documented and summarized.***

Piezoelectricity-continued

- Focused studies on wave propagation in piezoelectric plates are pioneered by ***Prof. Raymond D. Mindlin*** of Columbia University.
- The first paper on the late Mindlin plate theory was published in 1951 (R. D. Mindlin, Influence of rotatory inertia and shear on flexural motions of isotropic, elastic plates, *J. Appl. Mechanics*, **18**, 31-38, 1951).
- The Mindlin plate theory is presented by a monograph prepared for the US Army Signal Corps in 1955 and published in 2007 (R. D. Mindlin (edited by Jiashi Yang), *An Introduction to the Mathematical Theory of Vibrations of Elastic Plates*, World Scientific, 2007).
- Extensive studies on the high frequency vibrations of piezoelectric plates have been done for the quartz crystal industry by Profs. R. D. Mindlin, H. F. Tiersten, P. C. Y. Lee, and others.

Piezoelectricity-continued

- As a consultant to the Bell Telephone Laboratories, ***Prof. Harry F. Tiersten*** of Rensselaer trained engineers at the Piezoelectric Crystal Device Department there and the lecture notes have been published as an important reference on the fundamental theory and analytical techniques (H. F. Tiersten, *Linear Piezoelectric Plate Vibrations*, New York, Plenum Press, 1969).
- Prof. Tiersten has made important contributions to the quartz crystal device industry through his life-time research and training of engineers.

http://www.ieee-uffc.org/frequency_control/memoria.asp?name=tiersten

Piezoelectricity-continued

- Prof. ***Peter C. Y. Lee*** of Princeton started research on piezoelectric plate vibrations with Prof. Mindlin and continued with extensive contributions to the theoretical and practical problems in the analysis of quartz crystal resonators.
- ***The Lee plate theory*** (P. C. Y. Lee, J. D. Yu, and W.-S. Lin, A new two-dimensional theory for vibrations of piezoelectric crystal plates with electroded faces, *J. Appl. Phys.*, **83** (3), 1213 – 1223, 1998; P. C. Y. Lee, S. Syngellakis, and J. P. Hou, A two-dimensional theory for high-frequency vibrations of piezoelectric crystal plates with or without electrodes, *J. Appl. Phys.*, **61** (4), 1249 – 1262, 1987) takes the same approach as the Mindlin plate theory but with certain advantages.
- Many students of Prof. Lee are also active in piezoelectric acoustic wave device industry.

Future Trends

- Continuing and accelerating shrinkage in resonator size
- IC compatible fabrication process
- Quartz MEMS
- Multilayered thin film resonators (FBAR etc)
- New fabrication and processing technology
- All these technology require improved analysis and modeling based on existing (like Mindlin plate theory) or emerging theory (like nano- related) and sophisticated solutions techniques (like the finite element method) to provide design guidance with increased difficulties in prototyping and experiments.
- Besides, the fundamental theory and approximation solutions will be important in understanding the functioning mechanism and phenomena.

Piezoelectricity-continued

Research work on the high frequency vibrations of piezoelectric plates are still being performed with industrial support with major activities at:

- Prof. Yook-Kong Yong of Rutgers University.
  http://www.linkedin.com/pub/yook-kong-yong/4/a27/186
- Profs. Hitoshi Sekimoto and Yasuaki Watanabe of Tokyo Metropolitan University.
  http://ee-serv.eei.metro-u.ac.jp/faculty/y.watanabe/eng.php
  http://ee-serv.eei.metro-u.ac.jp/faculty/h.sekimoto/eng.php
- Prof. Ji Wang of Ningbo University.
  http://piezo.nbu.edu.cn/wangji/jiwangENS.PDF
- Prof. Jiashi Yang of University of Nebraska-Lincoln.
  http://www.unl.edu/ncmn/faculty/yang.shtml

提纲

1. 石英晶体谐振器的历史和趋势
2. 弹性波基础
3. 石英晶体
4. 无限大板的厚度振动
5. Mindlin板方程
6. 复杂因素

Wave Propagation

References on Wave Propagation in Piezoelectric Solids

1. H. F. Tiersten, *Linear Vibrations of Piezoelectric Plates,* New York: Plenum Press, 1969.
2. R. D. Mindlin, High frequency vibrations of piezoelectric crystal plates, *Int. J. Solids Struct.* **8**, 895-906, 1972.
3. R. D. Mindlin, Frequencies of piezoelectrically forced vibrations of electrode, doubly rotated, quartz plates, *Int. J. Solids Struct.* **20** (2), 141-157, 1984.
4. Jiashi Yang, *An Introduction to the Theory of Piezoelectricity*, Springer, 2005.
5. Jiashi Yang, *The Analysis of Piezoelectric Structure*, World Scientific, 2006.
6. B. A. Auld, *Acoustic Fields and Waves in Solids*, Krieger Publishing Company, 1990.
7. D. Royer and E. Dieulesaint, *Elastic Waves in Solids*, Springer, 2000.
8. R. D. Mindlin (JS Yang ed.), *An Introduction to the Mathematical Theory of Vibrations of Elastic Plates*, World Scientific, 2007.

Wave Propagation-continued

Field (gradient, kinematic) equations

$$S_{ij} = \frac{1}{2}\left(u_{i,j} + u_{j,i}\right), i, j = 1,2,3,$$

$$E_k = -\varphi_{,k}, k = 1,2,3,$$

where

u_i: displacements,

φ: electrical potential,

S_{ij}: strains,

E_k: electrical field.

Wave Propagation-continued

Divergent equations (differential equations of motion and charge equation)

$T_{ij,i} = \rho \ddot{u}_j, i, j = 1,2,3,$

$D_{k,k} = 0, k = 1,2,3,$

where

ρ: density of material,

T_{ij}: stresses,

D_k: electrical displacements.

Wave Propagation-continued

Constitutive (algebraic) equations

$$T_{ij} = c_{ijkl} S_{kl} - e_{kij} E_k,$$

$$D_i = e_{ijk} S_{jk} + \varepsilon_{ik} E_k, i, j, k, l = 1,2,3,$$

where

c_{ijkl} : elastic constants,

e_{kij} : piezoelectric constants,

ε_{ij} : dielectric constants.

Wave Propagation-continued

These equations are related to the ***enthalpy*** of a piezoelectric solid through

$$H = \frac{1}{2} c_{ijkl} S_{ij} S_{kl} - e_{ijk} E_i S_{jk} - \frac{1}{2} \varepsilon_{ij} E_i E_j ,$$

$$T_{ij} = \frac{\partial H}{\partial S_{ij}},$$

$$D_i = -\frac{\partial H}{\partial E_i}, i, j, k, l = 1,2,3.$$

Note the ***internal energy*** of a piezoelectric solid is

$$U = \frac{1}{2} c_{ijkl} S_{ij} S_{kl} + \frac{1}{2} \varepsilon_{ij} E_i E_j , i, j, k, l = 1,2,3.$$

Wave Propagation-continued

The above equations have 22 variables and 22 equations, representing a well-posed ***boundary value problem*** to be solved with proper ***boundary conditions for the mechanical and electrical variables***.

Finally, equations of motion of mechanical displacements and charge equation of electrical potential are given as

$$c_{ijkl}\,u_{k,li} + e_{kij}\,\varphi_{,ki} = \rho\ddot{u}_j,$$
$$e_{ikl}\,u_{k,li} - \varepsilon_{ik}\,\varphi_{,ki} = 0, i, j, k, l = 1,2,3.$$

提纲

1. 石英晶体谐振器的历史和趋势
2. 弹性波基础
3. 石英晶体
4. 无限大板的厚度振动
5. Mindlin板方程
6. 复杂因素

Quartz Crystal Materials

- The commonly used piezoelectric materials are crystals with certain special structures. For piezoelectric acoustic wave resonators, most popular materials are ***quartz crystal*** and ceramics.
- First of all, we adopt the abbreviated (compressed, contracted, compact) notations of stresses and strains along with material constants to give constitutive relations as (H. F. Tiersten, *Linear Vibrations of Piezoelectric Plates,* Plenum Press, 1969; R. D. Mindlin, *An Introduction to the Mathematical Theory of Vibrations of Elastic Plates*, World Scientific, 2007; ANSI/IEEE Std 176-1987, *IEEE Standard on Piezoelectricity*, IEEE, 1987.)

Quartz Crystal Materials - continued

$$T_p = c_{pq} S_q - e_{kp} E_k, p, q = 1,2,3,4,5,6, k = 1,2,3,$$
$$D_i = e_{iq} S_q + \varepsilon_{ik} E_k, i, k = 1,2,3.$$

The rules of correspondence of the subscripts are follows:

$$11 \rightarrow 1, 22 \rightarrow 2, 33 \rightarrow 3, 23 \rightarrow 4, 13 \rightarrow 5, 12 \rightarrow 6.$$

Earlier equations can be simplified with these newer notations.

Quartz Crystal Materials - continued

Material properties with general anisotropy

$$c_{pq} = \begin{bmatrix} c_{11} & c_{12} & c_{13} & c_{14} & c_{15} & c_{16} \\ c_{21} & c_{22} & c_{23} & c_{24} & c_{25} & c_{26} \\ c_{31} & c_{32} & c_{33} & c_{34} & c_{35} & c_{36} \\ c_{41} & c_{42} & c_{43} & c_{44} & c_{45} & c_{46} \\ c_{51} & c_{52} & c_{53} & c_{54} & c_{55} & c_{56} \\ c_{61} & c_{62} & c_{63} & c_{64} & c_{65} & c_{66} \end{bmatrix},$$

$$e_{kp} = \begin{bmatrix} e_{11} & e_{12} & e_{13} & e_{14} & e_{15} & e_{16} \\ e_{21} & e_{22} & e_{23} & e_{24} & e_{25} & e_{26} \\ e_{31} & e_{32} & e_{33} & e_{34} & e_{35} & e_{36} \end{bmatrix},$$

$$\varepsilon_{ij} = \begin{bmatrix} \varepsilon_{11} & \varepsilon_{12} & \varepsilon_{13} \\ \varepsilon_{21} & \varepsilon_{22} & \varepsilon_{23} \\ \varepsilon_{31} & \varepsilon_{32} & \varepsilon_{33} \end{bmatrix}.$$

Quartz Crystal Materials - continued

Most frequently used piezoelectric quartz crystal is the monoclinic Y-cut with 25 independent constants (H. F. Tiersten *Linear piezoelectric plate vibrations*, Plenum Press, 1969)

$$c_{pq} = \begin{bmatrix} c_{11} & c_{12} & c_{13} & c_{14} & & \\ c_{21} & c_{22} & c_{23} & c_{24} & & \\ c_{31} & c_{32} & c_{33} & c_{34} & & \\ c_{41} & c_{42} & c_{43} & c_{44} & & \\ & & & & c_{55} & c_{56} \\ & & & & c_{65} & c_{66} \end{bmatrix},$$

$$e_{kp} = \begin{bmatrix} e_{11} & e_{12} & e_{13} & e_{14} & & \\ & & & & e_{25} & e_{26} \\ & & & & e_{35} & e_{36} \end{bmatrix}, \varepsilon_{ij} = \begin{bmatrix} \varepsilon_{11} & & \\ & \varepsilon_{22} & \varepsilon_{23} \\ & \varepsilon_{32} & \varepsilon_{33} \end{bmatrix}.$$

Quartz Crystal Materials - continued

Current constants are from Bechmann (R. Bechmann, Elastic and piezoelectric constants of alpha-quartz, *Phys. Rev.*, 1060, 1958). For AT-cut of quartz crystal,

$$c = \begin{bmatrix} 86.74 & -8.25 & 27.15 & -3.66 & & \\ & 129.77 & -7.42 & 5.70 & & \\ & & 102.83 & 9.92 & & \\ & & & 38.61 & & \\ & SYM & & & 68.81 & 2.53 \\ & & & & & 29.01 \end{bmatrix} \times 10^9 \ \mathrm{N/m^2},$$

$$e = \begin{bmatrix} 0.171 & -0.152 & -0.0187 & 0.067 & & \\ & & & & 0.108 & -0.095 \\ & & & & -0.0761 & 0.067 \end{bmatrix} \mathrm{C/m^2},$$

$$\varepsilon = \begin{bmatrix} 39.21 & & \\ & 39.82 & 0.86 \\ & 0.86 & 40.42 \end{bmatrix} \times 10^{-12} \mathrm{C/Vm}, k_{26}^2 = \frac{e_{26}^2}{c_{66}\varepsilon_{22}} = 0.0078126.$$

Quartz Crystal Materials - continued

In addition to the constitutive relations given above, there are other forms of constitutive relations which are frequently encountered as

$$S_{ij} = s^{E}_{ijkl} T_{kl} + d_{kij} E_k,$$
$$D_i = d_{ikl} T_{kl} + \varepsilon^{T}_{ik} E_k;$$
$$S_{ij} = s^{D}_{ijkl} T_{kl} + g_{kij} D_k,$$
$$E_i = -g_{ikl} T_{kl} + \beta^{T}_{ik} D_k;$$
$$T_{ij} = C^{D}_{ijkl} S_{kl} - h_{kij} D_k,$$
$$E_i = -h_{ikl} S_{kl} + \beta^{S}_{ik} D_k.$$

The superscript E (D and T) implies constant electric field (electrical displacement field and stress field).

Quartz Crystal Materials - continued

By assuming the wave solutions as

$$u_j = A_i \exp\{\mathrm{i}[k(l_1x_1 + l_2x_2 + l_3x_3) - \omega t]\}, j = 1,2,3,$$

$$\varphi = \varphi_0 \exp\{\mathrm{i}[k(l_1x_1 + l_2x_2 + l_3x_3) - \omega t]\},$$

where

A_i: amplitudes of displacements,

φ_0: amplitude of electrical potential,

ω: vibration frequency,

t: time,

k: wavenumber,

l_j: wave propagation direction,

x_j: coordinates.

Quartz Crystal Materials - continued

Through eliminating the electrical potential φ_0, we have three equations for wave velocities as

$$\rho v^2 A_i = \bar{\Gamma}_{il} A_l,$$
$$\bar{\Gamma}_{il} = \bar{c}_{ijkl}\, l_j\, l_k,$$
$$\bar{c}_{ijkl} = c_{ijkl} + \frac{e_{kij}\, l_j\, l_k\, e_{klj}}{\varepsilon_{jk}\, l_j\, l_k}.$$

The ***Christoffel equation*** is

$$(\bar{\Gamma}_{il} - \rho v^2\, \delta_{il}) A_l = 0.$$

What we can obtain from these equations are the three velocities of plane waves. For most materials, there are longitudinal and shear waves velocity solutions from this equation.

http://en.wikipedia.org/wiki/Crystal_oscillator

提纲

1. 石英晶体谐振器的历史和趋势
2. 弹性波基础
3. 石英晶体
4. 无限大板的厚度振动
5. Mindlin板方程
6. 复杂因素

Thickness Vibrations

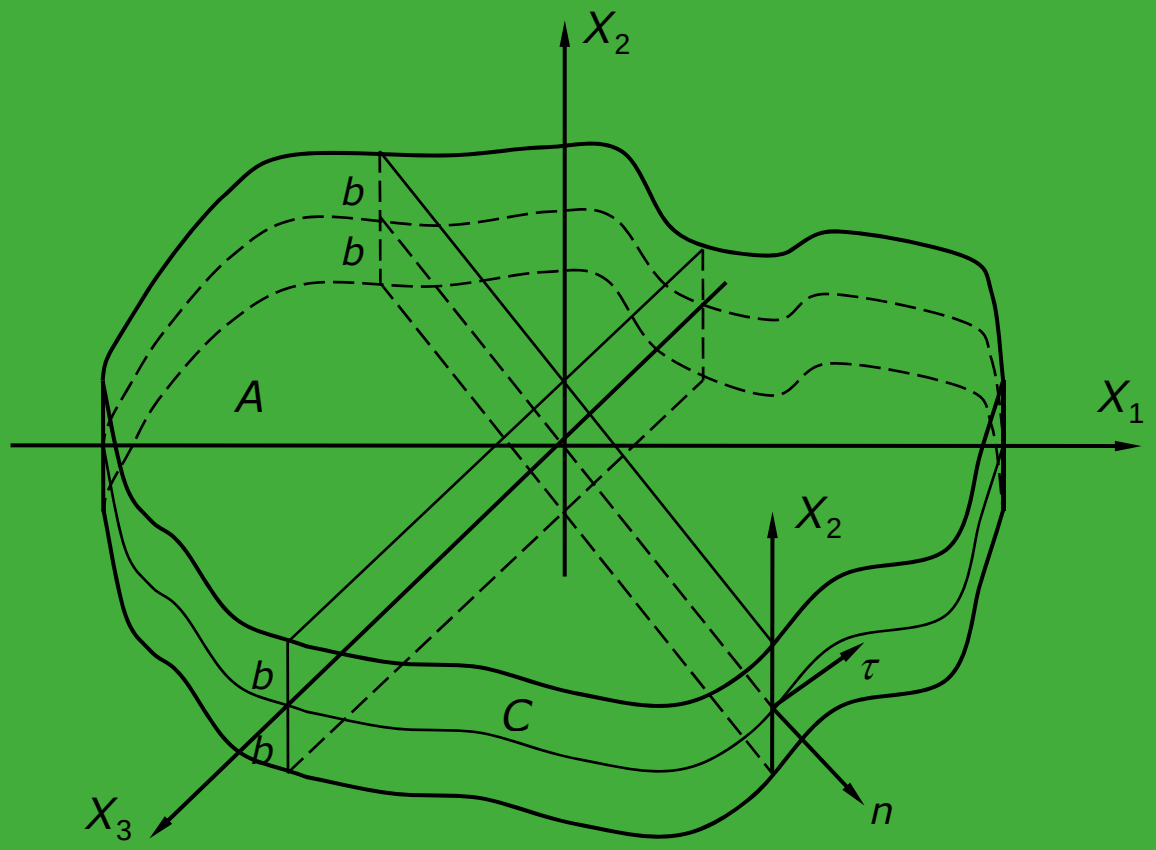


Fig. 1 A typical elastic plate with coordinates.

Thickness Vibrations - continued

For infinite plates, we assume there are only thickness vibration modes with displacements in the form of

$$u_j(x_2,t) = u_j(x_2)\mathrm{e}^{\mathrm{i}\omega t}, j = 1,2,3.$$

For monoclinic (Y-cut of quartz crystal) materials, we have equations of motion as

$$c_{66}u_{1,22} = \rho\ddot{u}_1,$$
$$c_{22}u_{2,22} + c_{24}u_{3,22} = \rho\ddot{u}_2,$$
$$c_{42}u_{2,22} + c_{44}u_{3,22} = \rho\ddot{u}_3,$$

and ***traction-free boundary conditions*** are

$$T_{21} = T_{22} = T_{23} = 0 \text{ at } x_2 = \pm b.$$

Thickness Vibrations – continued

It is clear that displacement u_1 is independent from other vibration modes. From the first equation, by assuming $u_1 = A_1 \sin \xi x_2 \, \mathrm{e}^{\mathrm{i}\omega t}$, we have

$$\omega^2 = \left(\frac{\pi}{2b}\right)^2 \frac{c_{66}}{\rho},$$

This is the thickness-shear vibration frequency. This equation has been used in the determination of the thickness of crystal plate with given frequency as

$$2b = \frac{1}{2f}\sqrt{\frac{c_{66}}{\rho}},$$

in resonator design. With known material constants $\rho = 2649\mathrm{kg/m}^3$ and $c_{66} = 29.01 \times 10^9 \mathrm{N/m}^2$, this has been known as frequency constants

$$2b = \frac{1654.6376}{f(\mathrm{MHz})} \ \mu\mathrm{m}.$$

Thickness Vibrations – continued

With the consideration of piezoelectricity, for a monoclinic material (rotated Y-cut quartz) under electrical field in the thickness direction, we have the differential equations as

$$c_{66}u_{1,22} + e_{26}\varphi_{,22} = \rho\ddot{u}_1,$$
$$c_{22}u_{2,22} + c_{24}u_{3,22} = \rho\ddot{u}_2,$$
$$c_{42}u_{2,22} + c_{44}u_{3,22} = \rho\ddot{u}_3,$$
$$e_{26}u_{1,22} - \varepsilon_{22}\varphi_{,22} = 0,$$

and the boundary conditions are

$$T_{21} = T_{22} = T_{23} = 0, \varphi = \pm\varphi_0 e^{i\omega t}, \text{at } x_2 = \pm b.$$

Thickness Vibrations – continued

It is clear that only displacement u_1 is coupled with the electrical field in the thickness-direction. We assume

$u_2 = u_3 = 0,$

$u_1(x_2, t) = u_1(x_2)e^{i\omega t},$

$\varphi(x_2, t) = \varphi(x_2)e^{i\omega t},$

and the substitution of above expressions into the differential equations will give

$$\left(c_{66} + \frac{e_{26}^2}{\varepsilon_{22}}\right)u_{1,22} + \rho\omega^2 u_1 = 0,$$

$$\varphi = \frac{e_{26}}{\varepsilon_{22}}u_1 + A_1 x_2 + A_2.$$

Thickness Vibrations – continued

Now we assume the displacement is antisymmetric function

$u_1 = A\sin\xi x_2 e^{i\omega t}$.

The differential equation is satisfied provided

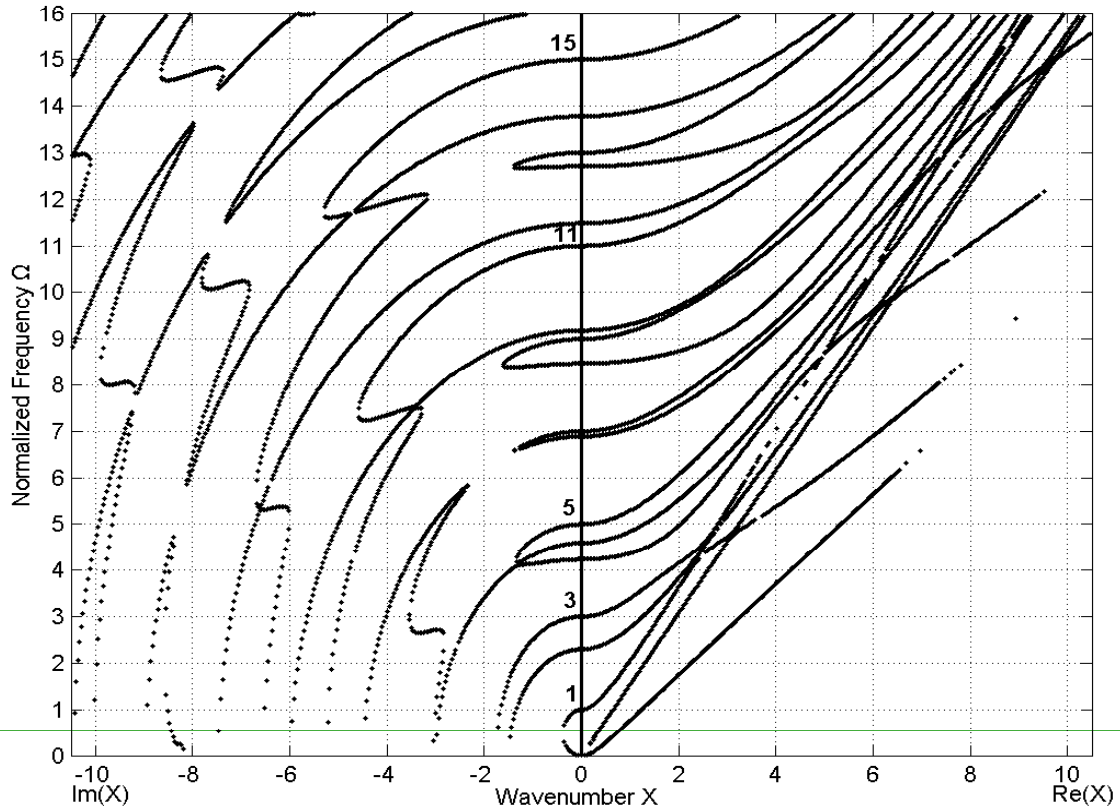
$$\bar{c}_{66}\xi^2 = \rho\omega^2, \bar{c}_{66} = c_{66} + \frac{e_{26}^2}{\varepsilon_{22}}.$$

The resonance frequency is obtained by setting the coefficient of the equations to vanish, ie

$$\tan\xi b = \frac{\bar{c}_{66}\varepsilon_{22}}{e_{26}^2}\xi b = \frac{\xi b}{k_{26}^2}.$$

This equation shows that wavelengths, consequently the frequencies, of the overtone thickness modes under piezoelectric driving are no longer integral fractions of fundamental mode. They have been modulated by the electromechanical coupling factor of the material.

Thickness Vibrations - continued



Dispersion relation of an AT-cut quartz crystal plate.

提纲

1. 石英晶体谐振器的历史和趋势
2. 弹性波基础
3. 石英晶体
4. 无限大板的厚度振动
5. Mindlin板方程
6. 复杂因素

Mindlin Plate Equations

The plate theories for the high frequency vibrations of plates are the ***Mindlin plate theory*** (R. D. Mindlin, *An Introduction to the Mathematical Theory of Vibrations of Elastic Plates*, World Scientific, 2007), ***Lee plate theory*** (P. C. Y. Lee, J. D. Yu, and W.-S. Lin, A new two-dimensional theory for vibrations of piezoelectric crystal plates with electroded faces, *J. Appl. Phys.*, **83** (3), 1213 – 1223, 1998; P. C. Y. Lee, S. Syngellakis, and J. P. Hou, A two-dimensional theory for high-frequency vibrations of piezoelectric crystal plates with or without electrodes, *J. Appl. Phys.*, **61** (4), 1249 – 1262, 1987), and ***Peach plate theory*** (R.C. Peach, A normal mode expansion for the piezoelectric plates and certain of its applications, *IEEE Trans. Ultrason., Ferroelect., Freq. Contr.* **35**, 593–611, 1988), which all are from the expansion of displacements in the thickness coordinate with basis functions representing the particular vibration modes we are interested in.

Mindlin Plate Equations- continued

The development of the Mindlin plate theory starts from the power series expansion of displacements in the form of (R. D. Mindlin, *An Introduction to the Mathematical Theory of Vibrations of Elastic Plates*, World Scientific, 2007)

$$u_j(x_1, x_2, x_3, t) = \sum_{n=0}^{\infty} u_j^{(n)}(x_1, x_3, t) x_2^n, j = 1,2,3.$$

Consequently, the strain components will be

$$S_{ij} = \sum_{n=0}^{\infty} S_{ij}^{(n)} x_2^n, S_{ij}^{(n)} = \frac{1}{2}\left[u_{i,j}^{(n)} + u_{j,i}^{(n)} + (n+1)\left(\delta_{2i} u_j^{(n+1)} + \delta_{2j} u_i^{(n+1)}\right)\right], i,j = 1,2,3.$$

Mindlin Plate Equations- continued

Since the variational equation of motion is

$$\int_V \left(T_{ij,i} - \rho \ddot{u}_j\right) \delta u_j \, dV = 0,$$

by substituting the displacement into the equation of motion and integrating over the thickness, we have

$$T_{ij,i}^{(n)} - nT_{2j}^{(n-1)} + F_j^{(n)} = \rho \sum_{m=0}^{\infty} B_{mn} \ddot{u}_j^{(m)},$$

where

$$T_{ij}^{(n)} = \sum_{m=0}^{\infty} B_{mn} c_{ijkl} S_{kl}^{(m)},$$

$$F_j^{(n)} = b^n \left[T_{2j}(b) - (-1)^n T_{2j}(-b)\right],$$

$$B_{mn} = \begin{cases} \dfrac{2b^{m+n+1}}{m+n+1}, & m+n \quad \text{even}, \\ 0, & m+n \quad \text{odd}. \end{cases}$$

Mindlin Plate Equations- continued

This also gives the two-dimensional constitutive relations with corrections as (Ji Wang, J-D Yu, and Y-K Yong, On the correction of higher-order Mindlin plate theory, *Int. J. Appl. Electromagnetics Mech.* **22**, 83-96, 2005.)

$$T_p^{(n)} = \sum_{m=0}^{\infty} B_{mn}\kappa_p^{(m)}\left\{c_{p1}u_{1,1}^{(m)} + c_{p2}\kappa_2^{(m)}(m+1)u_2^{(m+1)} + c_{p4}\kappa_4^{(m)}(m+1)u_3^{(m+1)} + c_{p5}u_3^{(m+1)} + c_{p6}\kappa_6^{(m)}\left[u_{2,1}^{(m)} + (m+1)u_1^{(m+1)}\right]\right\}.$$

Mindlin Plate Equations- continued

The ***boundary conditions*** for the Mindlin plate equations are that with the traction-free faces being considered, we need to prescribe either mechanical displacements $u_j^{(n)}(j = 1,2,3 \text{ and } n = 0,1,2,\ldots)$ or stresses $T_p^{(n)}(p = 1,2,3,4,5,6 \text{ and } n = 0,1,2,\cdots)$ on the cylindrical surfaces.

Mindlin Plate Equations- continued

As an example, the zeroth-order stresses for AT-cut quartz crystals are

$$T_1^{(0)} = 2b\left[c_{11}u_{1,1}^{(0)} + c_{12}u_2^{(1)} + c_{13}u_{3,3}^{(0)} + c_{14}\left(u_{2,3}^{(0)} + u_3^{(1)}\right)\right],$$

$$T_2^{(0)} = 2b\left[c_{21}u_{1,1}^{(0)} + c_{22}u_2^{(1)} + c_{23}u_{3,3}^{(0)} + c_{24}\left(u_{2,3}^{(0)} + u_3^{(1)}\right)\right],$$

$$T_3^{(0)} = 2b\left[c_{31}u_{1,1}^{(0)} + c_{32}u_2^{(1)} + c_{33}u_{3,3}^{(0)} + c_{34}\left(u_{2,3}^{(0)} + u_3^{(1)}\right)\right],$$

$$T_4^{(0)} = 2b\left[c_{41}u_{1,1}^{(0)} + c_{42}u_2^{(1)} + c_{43}u_{3,3}^{(0)} + c_{44}\left(u_{2,3}^{(0)} + u_3^{(1)}\right)\right],$$

$$T_5^{(0)} = 2b\left[c_{55}\left(u_{1,3}^{(0)} + u_{3,1}^{(0)}\right) + c_{56}\left(u_{2,1}^{(0)} + u_1^{(1)}\right)\right],$$

$$T_6^{(0)} = 2b\left[c_{65}\left(u_{1,3}^{(0)} + u_{3,1}^{(0)}\right) + c_{66}\left(u_{2,1}^{(0)} + u_1^{(1)}\right)\right];$$

Mindlin Plate Equations- continued

The first-order stresses are

$$T_1^{(1)} = \frac{2b^3}{3}\left(c_{11}u_{1,1}^{(1)} + c_{13}u_{3,3}^{(1)} + c_{14}u_{2,3}^{(1)}\right),$$

$$T_2^{(1)} = \frac{2b^3}{3}\left(c_{21}u_{1,1}^{(1)} + c_{23}u_{3,3}^{(1)} + c_{24}u_{2,3}^{(1)}\right),$$

$$T_3^{(1)} = \frac{2b^3}{3}\left(c_{31}u_{1,1}^{(1)} + c_{33}u_{3,3}^{(1)} + c_{34}u_{2,3}^{(1)}\right),$$

$$T_4^{(1)} = \frac{2b^3}{3}\left(c_{41}u_{1,1}^{(1)} + c_{43}u_{3,3}^{(1)} + c_{44}u_{2,3}^{(1)}\right),$$

$$T_5^{(1)} = \frac{2b^3}{3}\left[c_{55}(u_{1,3}^{(1)} + u_{3,1}^{(1)}) + c_{56}u_{2,1}^{(1)}\right],$$

$$T_6^{(1)} = \frac{2b^3}{3}\left[c_{65}(u_{1,3}^{(1)} + u_{3,1}^{(1)}) + c_{66}u_{2,1}^{(1)}\right].$$

Mindlin Plate Equations- continued

The zeroth- and first-order equations of motion are

$$T_{1,1}^{(0)} + T_{5,3}^{(0)} + F_1^{(0)} = 2b\rho\ddot{u}_1^{(0)},$$
$$T_{6,1}^{(0)} + T_{4,3}^{(0)} + F_2^{(0)} = 2b\rho\ddot{u}_2^{(0)},$$
$$T_{5,1}^{(0)} + T_{4,3}^{(0)} + F_3^{(0)} = 2b\rho\ddot{u}_3^{(0)};$$

$$T_{1,1}^{(1)} + T_{5,3}^{(1)} - T_6^{(0)} + F_1^{(1)} = \frac{2b^3}{3}\rho\ddot{u}_1^{(1)},$$
$$T_{6,1}^{(1)} + T_{4,3}^{(1)} - T_2^{(0)} + F_2^{(1)} = \frac{2b^3}{3}\rho\ddot{u}_2^{(1)},$$
$$T_{5,1}^{(1)} + T_{4,3}^{(1)} - T_4^{(0)} + F_3^{(1)} = \frac{2b^3}{3}\rho\ddot{u}_3^{(1)}.$$

Mindlin Plate Equations- continued

As an illustration of the corrected equations, we modify the zeroth-order equations with correction factors as

$$T_1^{(0)} = 2b\left[c_{11}u_{1,1}^{(0)} + c_{12}\kappa_2^{(0)}u_2^{(1)} + c_{13}u_{3,3}^{(0)} + c_{14}\kappa_4^{(0)}\left(u_{2,3}^{(0)} + u_3^{(1)}\right)\right],$$

$$T_2^{(0)} = 2b\kappa_2^{(0)}\left[c_{21}u_{1,1}^{(0)} + c_{22}\kappa_2^{(0)}u_2^{(1)} + c_{23}u_{3,3}^{(0)} + c_{24}\kappa_4^{(0)}\left(u_{2,3}^{(0)} + u_3^{(1)}\right)\right],$$

$$T_3^{(0)} = 2b\left[c_{31}u_{1,1}^{(0)} + c_{32}\kappa_2^{(0)}u_2^{(1)} + c_{33}u_{3,3}^{(0)} + c_{34}\kappa_4^{(0)}\left(u_{2,3}^{(0)} + u_3^{(1)}\right)\right],$$

$$T_4^{(0)} = 2b\kappa_4^{(0)}\left[c_{41}u_{1,1}^{(0)} + c_{42}\kappa_2^{(0)}u_2^{(1)} + c_{43}u_{3,3}^{(0)} + c_{44}\kappa_4^{(0)}\left(u_{2,3}^{(0)} + u_3^{(1)}\right)\right],$$

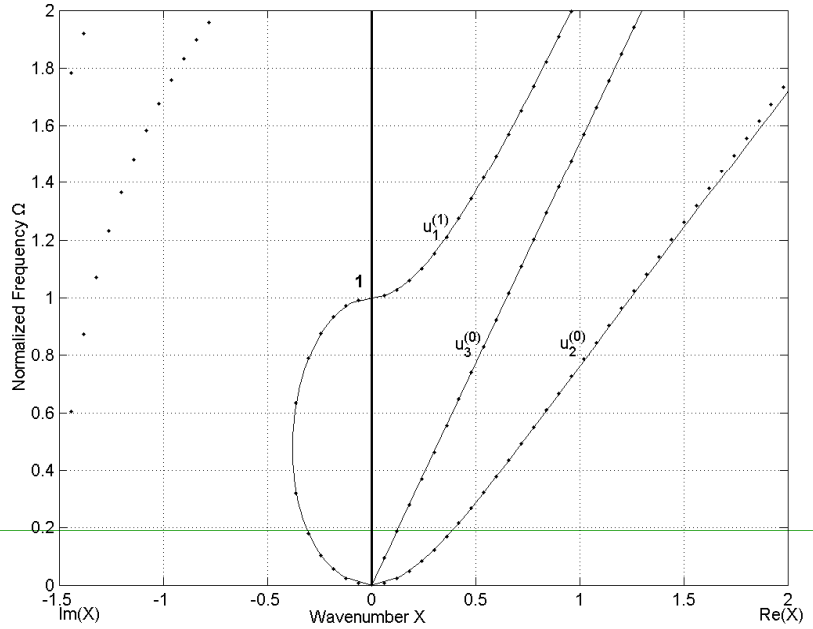
$$T_5^{(0)} = 2b\left[c_{55}\left(u_{1,3}^{(0)} + u_{3,1}^{(0)}\right) + c_{56}\kappa_6^{(0)}\left(\alpha u_{2,1}^{(0)} + u_1^{(1)}\right)\right],$$

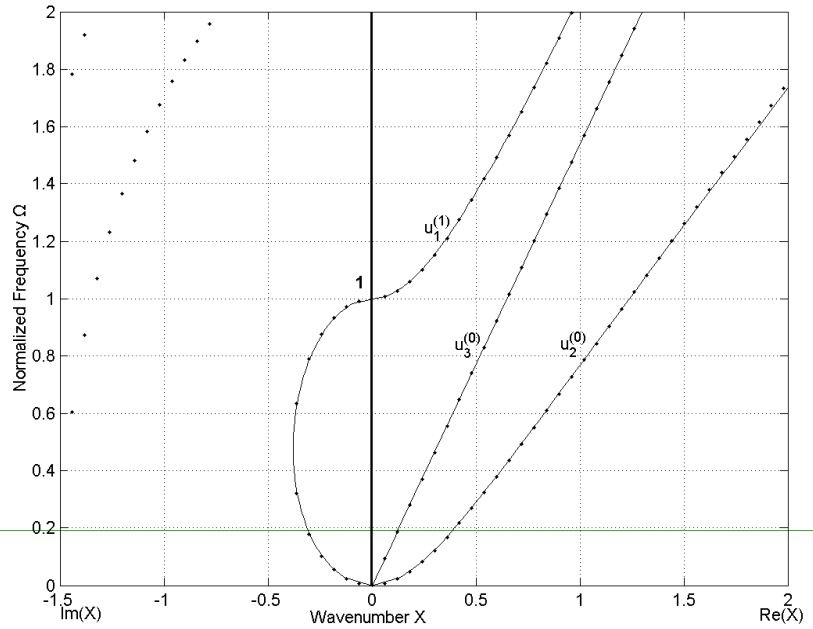
$$T_6^{(0)} = 2b\kappa_6^{(0)}\left[c_{65}\left(u_{1,3}^{(0)} + u_{3,1}^{(0)}\right) + c_{66}\kappa_6^{(0)}\left(\alpha u_{2,1}^{(0)} + u_1^{(1)}\right)\right];$$

where the correction factors are

$$\kappa_2^{(0)} = \kappa_4^{(0)} = \kappa_6^{(0)} = \sqrt{\frac{\pi^2}{12}} = 0.90689968, \alpha = 1.02.$$

Mindlin Plate Equations- continued





Comparison of dispersion relations from the exact solutions and the Mindlin plate equations with correction.

Mindlin Plate Equations- continued

The essence of the straight-crested wave assumption is that the displacements have one spatial variable for much aggressive simplification. First of all, we start with the assumption of the thickness-shear displacement as

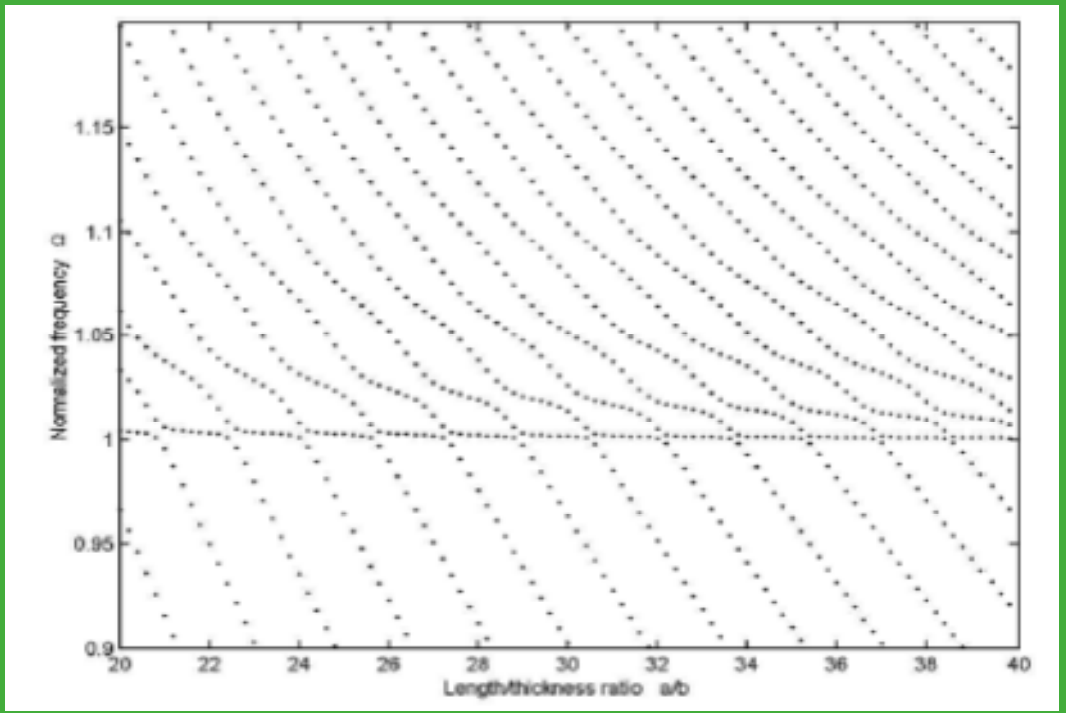
$$u_1^{(1)} = A_1 \cos\xi x_1 \mathrm{e}^{\mathrm{i}\omega t},$$

for x_1 coordinate in the center of plate. It implies that the thickness-shear displacement is confined in the center of the plate, a fact which is also viewed as the unique energy trapping feature. Then through the coupled equations, we can easily obtain other displacements as

$$u_2^{(0)} = A_2 \sin\xi x_1 \mathrm{e}^{\mathrm{i}\omega t},$$
$$u_3^{(0)} = A_3 \sin\xi x_1 \mathrm{e}^{\mathrm{i}\omega t},$$
$$u_3^{(1)} = A_4 \sin\xi x_1 \mathrm{e}^{\mathrm{i}\omega t}.$$

Mindlin Plate Equations- continued

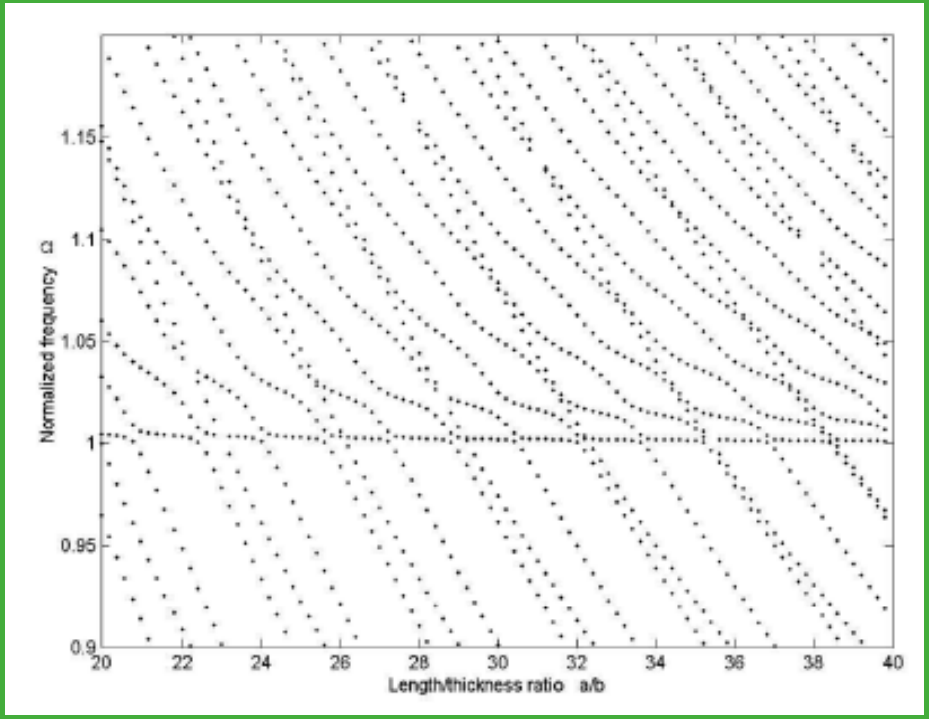
Thickness-shear and flexural vibrations



Ji Wang and Wenhua Zhao, The Determination of the Optimal Length of Crystal Blanks in Quartz Crystal Resonators, *IEEE Transactions on Ultrasonics, Ferroelectrics, and Frequency Control*, **52** (11), 2023-2030, 2005.

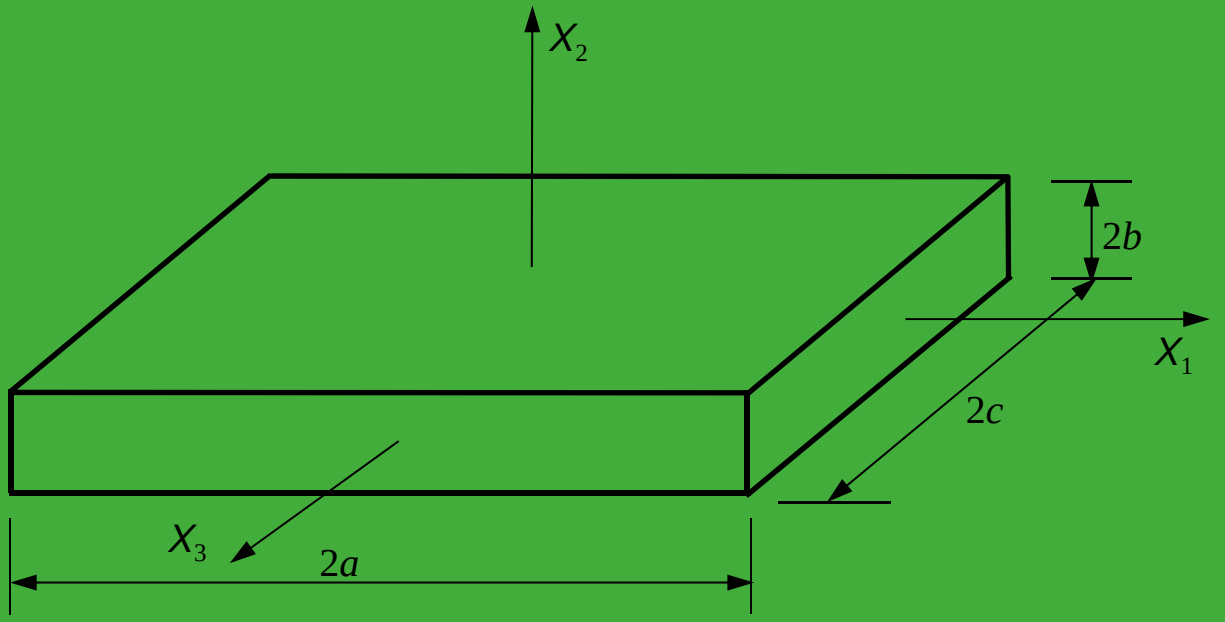
Mindlin Plate Equations- continued

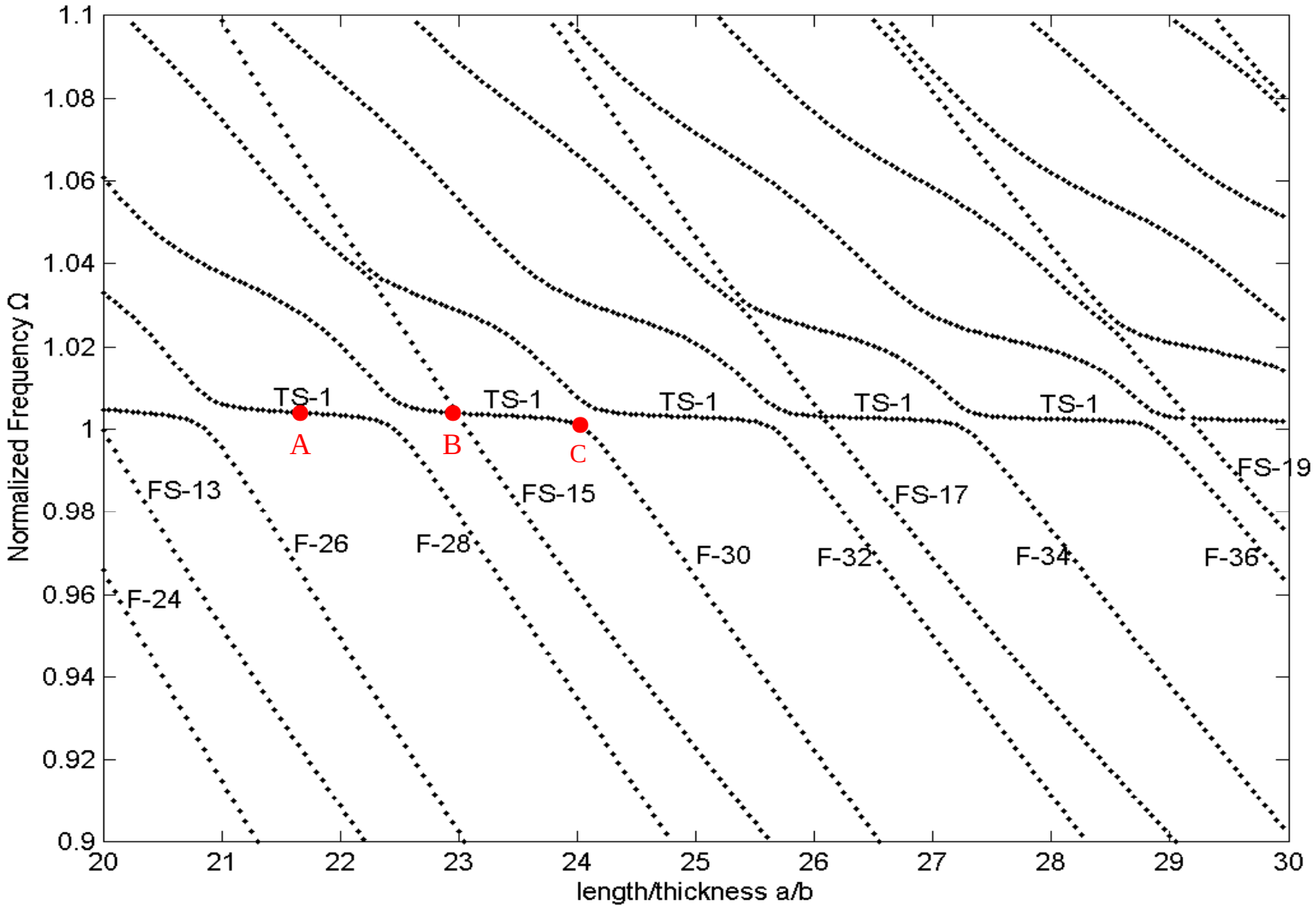
Thickness-shear, flexural , and face-shear vibrations

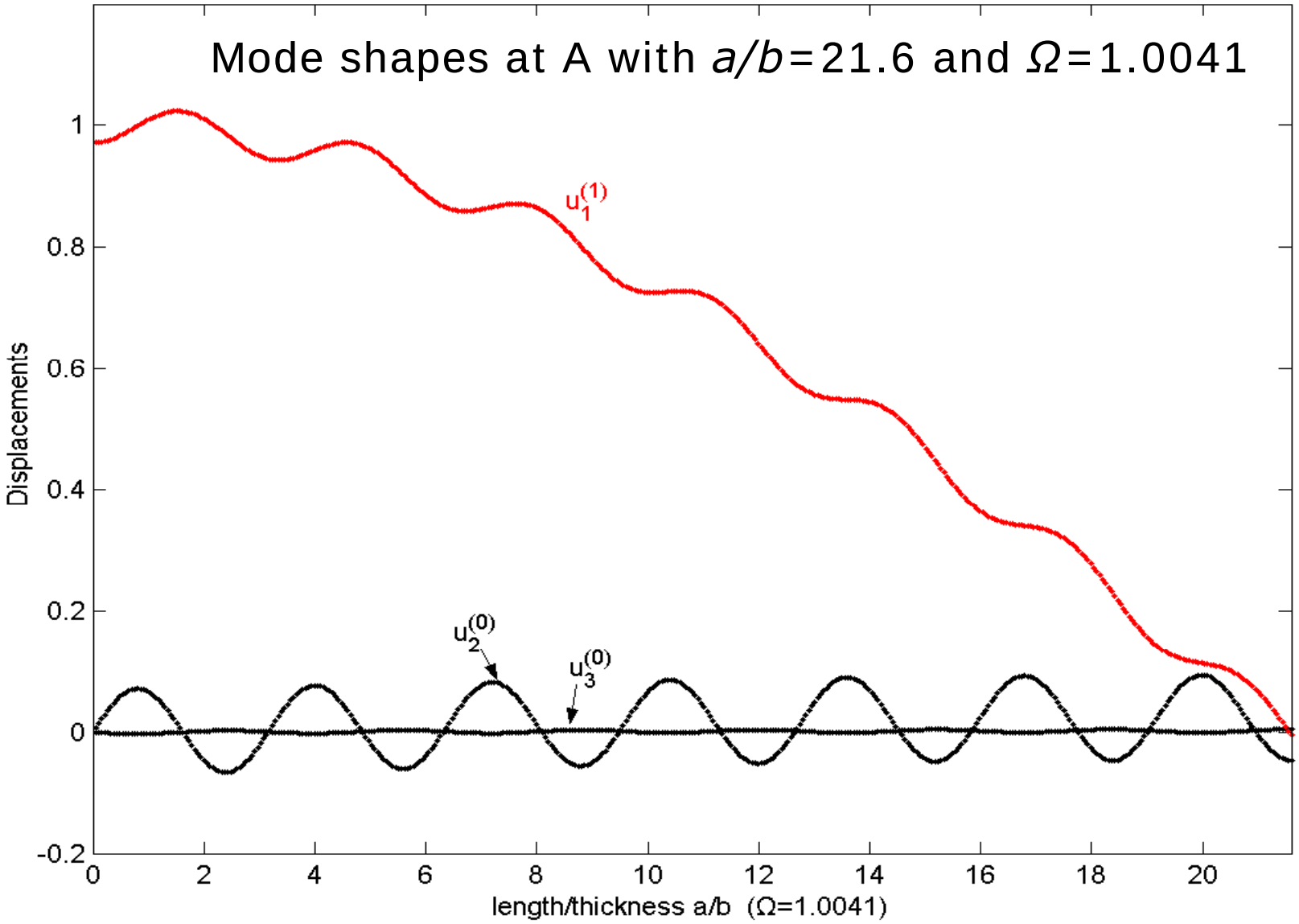


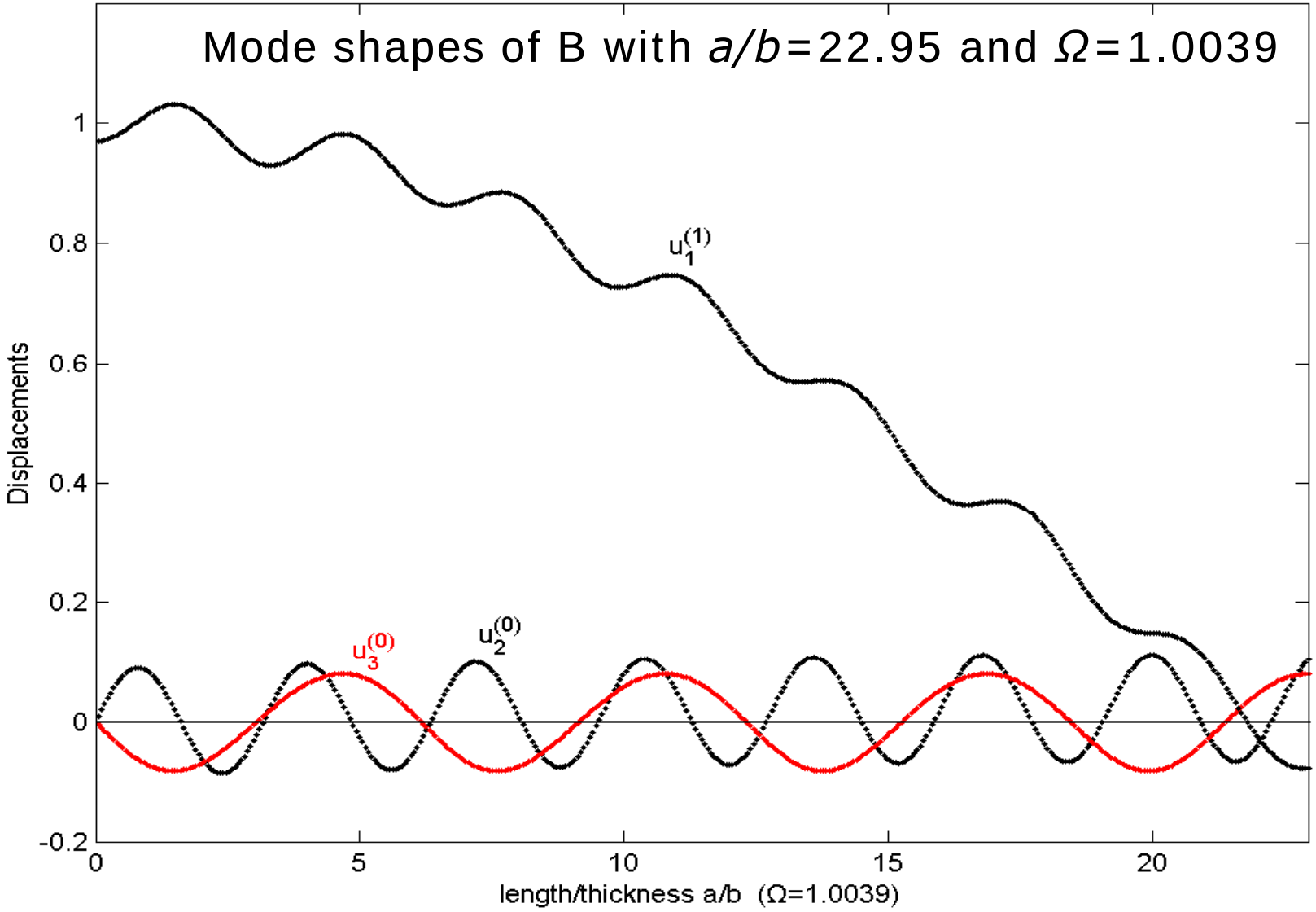
Ji Wang and Wenhua Zhao, The Determination of the Optimal Length of Crystal Blanks in Quartz Crystal Resonators, *IEEE Transactions on Ultrasonics, Ferroelectrics, and Frequency Control*, **52** (11), 2023-2030, 2005.

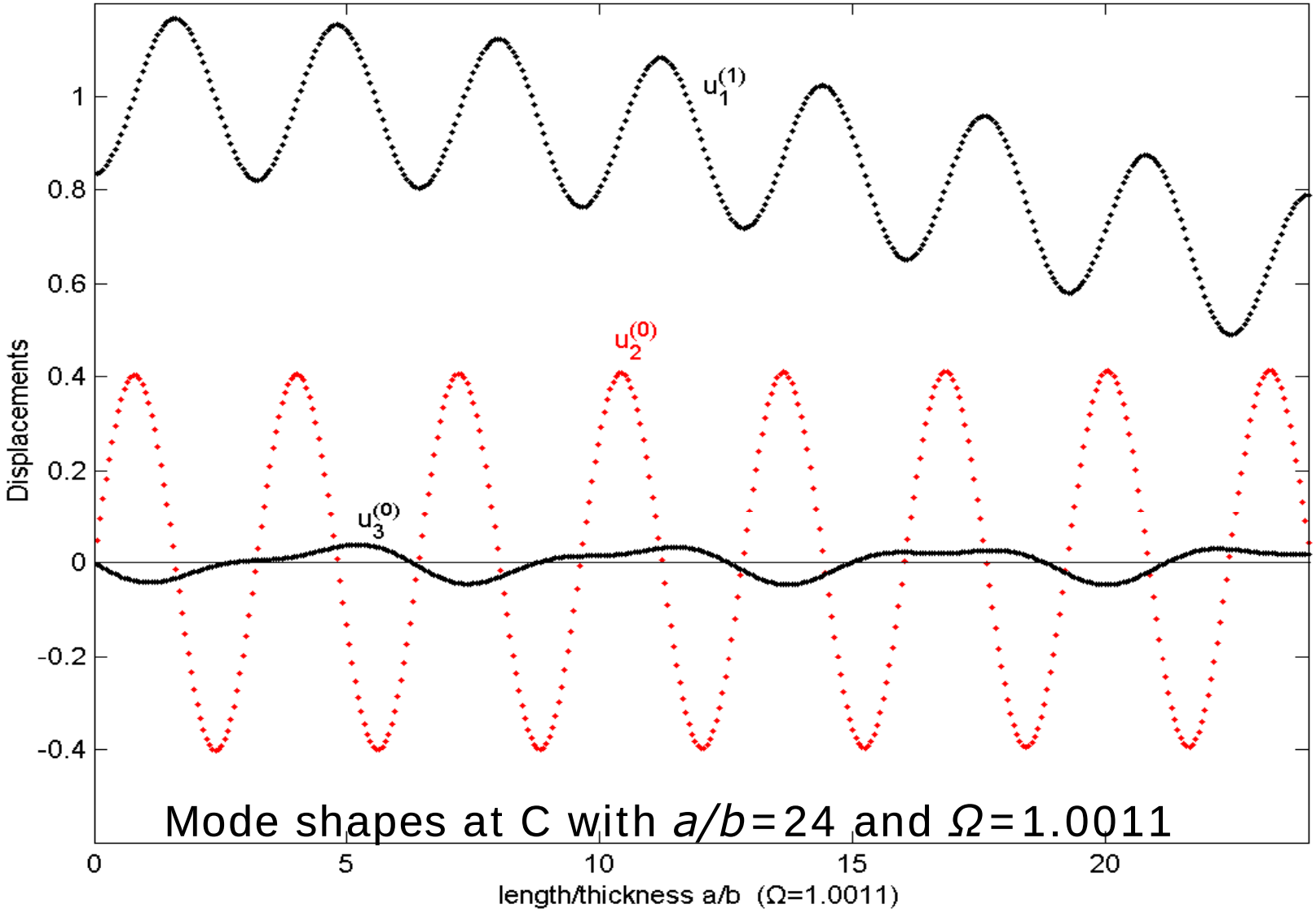
A rectangular plate for vibration analysis




Normalized Frequency Ω
length/thickness a/b
1.1
1.08
1.06
1.04
1.02
1
0.98
0.96
0.94
0.92
0.9
20
21
22
23
24
25
26
27
28
29
30
TS-1
TS-1
TS-1
TS-1
TS-1
A
B
C
FS-13
FS-15
FS-17
FS-19
F-24
F-26
F-28
F-30
F-32
F-34
F-36


Mode shapes at A with a/b=21.6 and Ω=1.0041
Displacements
length/thickness a/b (Ω=1.0041)
u1(1)
u2(0)
u3(0)
1
0.8
0.6
0.4
0.2
0
-0.2
0
2
4
6
8
10
12
14
16
18
20


Mode shapes of B with a/b=22.95 and Ω=1.0039
Displacements
length/thickness a/b (Ω=1.0039)
$u_1^{(1)}$
$u_2^{(0)}$
$u_3^{(0)}$
1
0.8
0.6
0.4
0.2
0
-0.2
0
5
10
15
20



Mode shapes at C with $a/b=24$ and $\Omega=1.0011$

Mindlin Plate Equations- continued

With the frequency spectra, we can always find the optimal parameters of a plate. From the spectra, the best plate length will be the middle of a span between two crossings by the flexural frequencies. With the one-dimensional solutions of the coupled thickness-shear and flexural modes, we can get the optimal length of an AT-cut quartz crystal blank as (Ji Wang and Wenhua Zhao, The Determination of the Optimal Length of Crystal Blanks in Quartz Crystal Resonators, *IEEE Transactions on Ultrasonics, Ferroelectrics, and Frequency Control*, 52 (11), 2023-2030, 2005.)

$$\frac{a}{b} = \left(n + \frac{1}{2}\right) 1.6056, n = 1, 2, 3, 4, \cdots, N.$$

This can be used as the initial design. More completed calculations have been carried out with equations of more coupled modes.

Overtone Mode Analysis

- There are many overtone mode quartz crystal resonators with wide applications.
- Our research proves that the Mindlin plate equations can also be extended to overtone vibration analysis.
- Corrected fifth-order Mindlin plate equations have been presented through our research.
- The overtone vibration analysis is doen with the fifth-order equations.

Fifth-order Mindlin plate equations

For traction-free plate, the Mindlin plate equations of motion for straight-crested waves with thickness-shear vibration modes up to the fifth-order are

$$T_{6,1}^{(0)} = 2b\rho\ddot{\phi}_2^{(0)} + \frac{2b^3}{3}\rho\ddot{\phi}_2^{(2)} + \frac{2b^5}{5}\rho\ddot{\phi}_2^{(4)}, \qquad T_{5,1}^{(0)} = 2b\rho\ddot{\phi}_3^{(0)} + \frac{2b^3}{3}\rho\ddot{\phi}_3^{(2)} + \frac{2b^5}{5}\rho\ddot{\phi}_3^{(4)},$$

$$T_{1,1}^{(1)} - T_6^{(0)} = \frac{2b^3}{3}\rho\ddot{\phi}_1^{(1)} + \frac{2b^5}{5}\rho\ddot{\phi}_1^{(3)} + \frac{2b^7}{7}\rho\ddot{\phi}_1^{(5)}, \quad T_{6,1}^{(2)} - 2T_2^{(1)} = \frac{2b^3}{3}\rho\ddot{\phi}_2^{(0)} + \frac{2b^5}{5}\rho\ddot{\phi}_2^{(2)} + \frac{2b^7}{7}\rho\ddot{\phi}_2^{(4)},$$

$$T_{5,1}^{(2)} - 2T_4^{(1)} = \frac{2b^3}{3}\rho\ddot{\phi}_3^{(0)} + \frac{2b^5}{5}\rho\ddot{\phi}_3^{(2)} + \frac{2b^7}{7}\rho\ddot{\phi}_3^{(4)}, T_{1,1}^{(3)} - 3T_6^{(2)} = \frac{2b^5}{5}\rho\ddot{\phi}_1^{(1)} + \frac{2b^7}{7}\rho\ddot{\phi}_1^{(3)} + \frac{2b^9}{9}\rho\ddot{\phi}_1^{(5)},$$

$$T_{6,1}^{(4)} - 4T_2^{(3)} = \frac{2b^5}{5}\rho\ddot{\phi}_2^{(0)} + \frac{2b^7}{7}\rho\ddot{\phi}_2^{(2)} + \frac{2b^9}{9}\rho\ddot{\phi}_2^{(4)}, T_{5,1}^{(4)} - 4T_4^{(3)} = \frac{2b^5}{5}\rho\ddot{\phi}_3^{(0)} + \frac{2b^7}{7}\rho\ddot{\phi}_3^{(2)} + \frac{2b^9}{9}\rho\ddot{\phi}_3^{(4)},$$

$$T_{1,1}^{(5)} - 5T_6^{(4)} = \frac{2b^7}{7}\rho\ddot{\phi}_1^{(1)} + \frac{2b^9}{9}\rho\ddot{\phi}_1^{(3)} + \frac{2b^{11}}{11}\rho\ddot{\phi}_1^{(5)}.$$

Fifth-order Mindlin plate equations

Two-dimensional stresses of AT-cut quartz crystals are given in displacements as

$$T_5^{(0)} = 2b\kappa_5^{(0)}\left[c_{55}u_{3,1}^{(0)} + c_{56}\kappa_6^{(0)}\left(u_{2,1}^{(0)} + u_1^{(1)}\right)\right] + \frac{2b^3}{3}\kappa_5^{(2)}\left[c_{55}u_{3,1}^{(2)} + c_{56}\kappa_6^{(2)}\left(u_{2,1}^{(2)} + 3u_1^{(3)}\right)\right]$$
$$+ \frac{2b^5}{5}\kappa_5^{(4)}\left[c_{55}u_{3,1}^{(4)} + c_{56}\kappa_6^{(4)}\left(u_{2,1}^{(4)} + 5u_1^{(5)}\right)\right],$$

$$T_6^{(0)} = 2b\kappa_6^{(0)}\left[c_{65}u_{3,1}^{(0)} + c_{66}\kappa_6^{(0)}\left(u_{2,1}^{(0)} + u_1^{(1)}\right)\right] + \frac{2b^3}{3}\kappa_6^{(2)}\left[c_{65}u_{3,1}^{(2)} + c_{66}\kappa_6^{(2)}\left(u_{2,1}^{(2)} + 3u_1^{(3)}\right)\right]$$
$$+ \frac{2b^5}{5}\kappa_6^{(4)}\left[c_{65}u_{3,1}^{(4)} + c_{66}\kappa_6^{(4)}\left(u_{2,1}^{(4)} + 5u_1^{(5)}\right)\right],$$

Fifth-order Mindlin plate equations

$$T_1^{(1)} = \frac{2b^3}{3}\kappa_1^{(1)}\left(c_{11}u_{1,1}^{(1)} + 2c_{12}\kappa_2^{(1)}u_2^{(2)} + 2c_{14}\kappa_4^{(1)}u_3^{(2)}\right) + \frac{2b^5}{5}\kappa_1^{(3)}\left(c_{11}u_{1,1}^{(3)} + 4c_{12}\kappa_2^{(3)}u_2^{(4)}\right)$$
$$+ \frac{8b^5}{5}\kappa_1^{(3)}c_{14}\kappa_4^{(3)}u_3^{(4)} + \frac{2b^7}{7}\kappa_1^{(5)}c_{11}u_{1,1}^{(5)},$$

$$T_2^{(1)} = \frac{2b^3}{3}\kappa_2^{(1)}\left(c_{21}u_{1,1}^{(1)} + 2c_{22}\kappa_2^{(1)}u_2^{(2)} + 2c_{24}\kappa_4^{(1)}u_3^{(2)}\right) + \frac{2b^5}{5}\kappa_2^{(3)}\left(c_{21}u_{1,1}^{(3)} + 4c_{22}\kappa_2^{(3)}u_2^{(4)}\right)$$
$$+ \frac{8b^5}{5}\kappa_2^{(3)}c_{24}\kappa_4^{(3)}u_3^{(4)} + \frac{2b^7}{7}\kappa_2^{(5)}c_{21}u_{1,1}^{(5)},$$

$$T_4^{(1)} = \frac{2b^3}{3}\kappa_4^{(1)}\left(c_{41}u_{1,1}^{(1)} + 2c_{42}\kappa_2^{(1)}u_2^{(2)} + 2c_{44}\kappa_4^{(1)}u_3^{(2)}\right) + \frac{2b^5}{5}\kappa_4^{(3)}\left(c_{41}u_{1,1}^{(3)} + 4c_{42}\kappa_2^{(3)}u_2^{(4)}\right)$$
$$+ \frac{8b^5}{5}\kappa_4^{(3)}c_{44}\kappa_4^{(3)}u_3^{(4)} + \frac{2b^7}{7}\kappa_4^{(5)}c_{41}u_{1,1}^{(5)},$$

Fifth-order Mindlin plate equations

$$T_5^{(2)}=\frac{2b^3}{3}\kappa_5^{(0)}\left[c_{55}u_{3,1}^{(0)}+c_{56}\kappa_6^{(0)}\left(u_{2,1}^{(0)}+u_1^{(1)}\right)\right]+\frac{2b^5}{5}\kappa_5^{(2)}\left[c_{55}u_{3,1}^{(2)}+c_{56}\kappa_6^{(2)}\left(u_{2,1}^{(2)}+3u_1^{(3)}\right)\right]$$
$$+\frac{2b^7}{7}\kappa_5^{(4)}\left[c_{55}u_{3,1}^{(4)}+c_{56}\kappa_6^{(4)}\left(u_{2,1}^{(4)}+5u_1^{(5)}\right)\right],$$

$$T_6^{(2)}=\frac{2b^3}{3}\kappa_6^{(0)}\left[c_{65}u_{3,1}^{(0)}+c_{66}\kappa_6^{(0)}\left(u_{2,1}^{(0)}+u_1^{(1)}\right)\right]+\frac{2b^5}{5}\kappa_6^{(2)}\left[c_{65}u_{3,1}^{(2)}+c_{66}\kappa_6^{(2)}\left(u_{2,1}^{(2)}+3u_1^{(3)}\right)\right]$$
$$+\frac{2b^7}{7}\kappa_6^{(4)}\left[c_{65}u_{3,1}^{(4)}+c_{66}\kappa_6^{(4)}\left(u_{2,1}^{(4)}+5u_1^{(5)}\right)\right],$$

$$T_1^{(3)}=\frac{2b^5}{5}\kappa_1^{(1)}\left(c_{11}u_{1,1}^{(1)}+2c_{12}\kappa_2^{(1)}u_2^{(2)}+2c_{14}\kappa_4^{(1)}u_3^{(2)}\right)+\frac{2b^7}{7}\kappa_1^{(3)}\left(c_{11}u_{1,1}^{(3)}+4c_{12}\kappa_2^{(3)}u_2^{(4)}\right)$$
$$+\frac{8b^7}{7}\kappa_1^{(3)}c_{14}\kappa_4^{(3)}u_3^{(4)}+\frac{2b^9}{9}\kappa_1^{(5)}c_{11}u_{1,1}^{(5)},$$

Fifth-order Mindlin plate equations

$$T_2^{(3)}=\frac{2b^5}{5}\kappa_2^{(1)}\left(c_{21}u_{1,1}^{(1)}+2c_{22}\kappa_2^{(1)}u_2^{(2)}+2c_{24}\kappa_4^{(1)}u_3^{(2)}\right)+\frac{2b^7}{7}\kappa_2^{(3)}\left(c_{21}u_{1,1}^{(3)}+4c_{22}\kappa_2^{(3)}u_2^{(4)}\right)$$
$$+\frac{8b^7}{7}\kappa_2^{(3)}c_{24}\kappa_4^{(3)}u_3^{(4)}+\frac{2b^9}{9}\kappa_2^{(5)}c_{21}u_{1,1}^{(5)},$$

$$T_4^{(3)}=\frac{2b^5}{5}\kappa_4^{(1)}\left(c_{41}u_{1,1}^{(1)}+2c_{42}\kappa_2^{(1)}u_2^{(2)}+2c_{44}\kappa_4^{(1)}u_3^{(2)}\right)+\frac{2b^7}{7}\kappa_4^{(3)}\left(c_{41}u_{1,1}^{(3)}+4c_{42}\kappa_2^{(3)}u_2^{(4)}\right)$$
$$+\frac{8b^7}{7}\kappa_4^{(3)}c_{44}\kappa_4^{(3)}u_3^{(4)}+\frac{2b^9}{9}\kappa_4^{(5)}c_{41}u_{1,1}^{(5)},$$

$$T_5^{(4)}=\frac{2b^4}{5}\kappa_5^{(0)}\left[c_{55}u_{3,1}^{(0)}+c_{56}\kappa_6^{(0)}\left(u_{2,1}^{(0)}+u_1^{(1)}\right)\right]+\frac{2b^7}{7}\kappa_5^{(2)}\left[c_{55}u_{3,1}^{(2)}+c_{56}\kappa_6^{(2)}\left(u_{2,1}^{(2)}+3u_1^{(3)}\right)\right]$$
$$+\frac{2b^9}{9}\kappa_5^{(4)}\left[c_{55}u_{3,1}^{(4)}+c_{56}\kappa_6^{(4)}\left(u_{2,1}^{(4)}+5u_1^{(5)}\right)\right],$$

Fifth-order Mindlin plate equations

$$T_6^{(4)} = \frac{2b^5}{5}\kappa_6^{(0)}\left[c_{65}u_{3,1}^{(0)} + c_{66}\kappa_6^{(0)}\left(u_{2,1}^{(0)} + u_1^{(1)}\right)\right] + \frac{2b^7}{7}\kappa_6^{(2)}\left[c_{65}u_{3,1}^{(2)} + c_{66}\kappa_6^{(2)}\left(u_{2,1}^{(2)} + 3u_1^{(3)}\right)\right]$$

$$+ \frac{2b^9}{9}\kappa_6^{(4)}\left[c_{65}u_{3,1}^{(4)} + c_{66}\kappa_6^{(4)}\left(u_{2,1}^{(4)} + 5u_1^{(5)}\right)\right],$$

$$T_1^{(5)} = \frac{2b^7}{7}\kappa_1^{(1)}\left(c_{11}u_{1,1}^{(1)} + 2c_{12}\kappa_2^{(1)}u_2^{(2)} + 2c_{14}\kappa_4^{(1)}u_3^{(2)}\right) + \frac{2b^9}{9}\kappa_1^{(3)}\left(c_{11}u_{1,1}^{(3)} + 4c_{12}\kappa_2^{(3)}u_2^{(4)}\right)$$

$$+ \frac{8b^9}{9}\kappa_1^{(3)}c_{14}\kappa_4^{(3)}u_3^{(4)} + \frac{2b^{11}}{11}\kappa_1^{(5)}c_{11}u_{1,1}^{(5)}.$$

Fifth-order Mindlin plate equations

The *correction factors* for accurate cut-off frequencies of the thickness-shear modes in the fifth-order plate theory are

$$\kappa_2^{(0)}=\kappa_4^{(0)}=\kappa_6^{(0)}=0.95236838,\quad \kappa_2^{(1)}=\kappa_4^{(1)}=\kappa_6^{(1)}=0.85873296,$$

$$\kappa_2^{(2)}=\kappa_4^{(2)}=\kappa_6^{(2)}=0.81748736,\quad \kappa_2^{(3)}=\kappa_4^{(3)}=\kappa_6^{(3)}=0.74774876,$$

$$\kappa_2^{(4)}=\kappa_4^{(4)}=\kappa_6^{(4)}=0.73240723,$$

$$\kappa_1^{(0)}=\kappa_3^{(0)}=\kappa_5^{(0)}=1,\qquad \kappa_1^{(1)}=\kappa_3^{(1)}=\kappa_5^{(1)}=1,$$

$$\kappa_1^{(2)}=\kappa_3^{(2)}=\kappa_5^{(2)}=1,\qquad \kappa_1^{(3)}=\kappa_3^{(3)}=\kappa_5^{(3)}=\kappa_1^{(5)}=1.$$

Fifth-order Mindlin plate equations

To calculate the dispersion relation for a plate shown in Fig.1, we consider displacements taking the straight-crested wave form

$$u_2^{(0)} = A_1 \sin \xi x_1 e^{i\omega t}, \quad u_3^{(0)} = A_2 \sin \xi x_1 e^{i\omega t}, \quad u_1^{(1)} = \frac{A_3}{b} \cos \xi x_1 e^{i\omega t},$$

$$u_2^{(2)} = \frac{A_4}{b^2} \sin \xi x_1 e^{i\omega t}, \quad u_3^{(2)} = \frac{A_5}{b^2} \sin \xi x_1 e^{i\omega t}, \quad u_1^{(3)} = \frac{A_6}{b^3} \cos \xi x_1 e^{i\omega t},$$

$$u_2^{(4)} = \frac{A_7}{b^4} \sin \xi x_1 e^{i\omega t}, \quad u_3^{(4)} = \frac{A_8}{b^4} \sin \xi x_1 e^{i\omega t}, \quad u_1^{(5)} = \frac{A_9}{b^5} \cos \xi x_1 e^{i\omega t}.$$

Fifth-order Mindlin plate equations

By substituting displacements back into stresses, then equations of motion, we can obtain the dispersion relation of an AT-cut quartz crystal plate. We compare the dispersion curves by the 3-D equations and by the fifth-order 2-D equations in Fig.2. This serves as a foundation for the future applications of these equations.

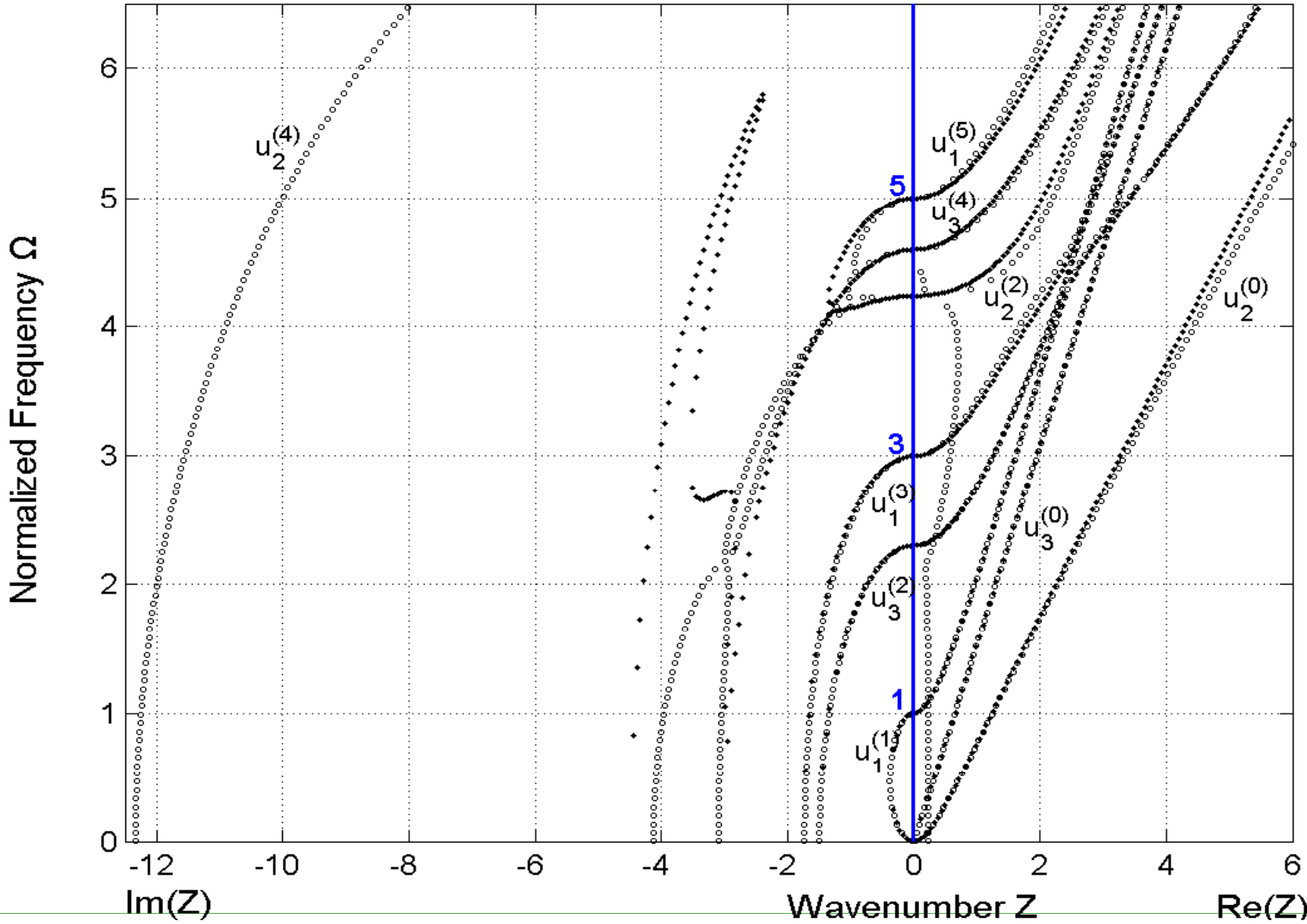


Fig. 2 Comparison of dispersion curves of an AT-cut quartz plate. Dots are predicted by the 3-D equations and circles by the fifth-order 2-D equations.

Frequency spectra

In order to calculate the frequency dependence on plate size like the length with straight-crested wave solutions, we can obtain displacements as

$$u_2^{(0)}=\sum_{r=1}^{9}\alpha_{1r}A_{9r}\sin\left(\frac{Z_r\pi}{2}\frac{x_1}{b}\right),\quad u_3^{(0)}=\sum_{r=1}^{9}\alpha_{2r}A_{9r}\sin\left(\frac{Z_r\pi}{2}\frac{x_1}{b}\right),\quad u_1^{(1)}=\sum_{r=1}^{9}\alpha_{3r}\frac{A_{9r}}{b}\cos\left(\frac{Z_r\pi}{2}\frac{x_1}{b}\right),$$

$$u_2^{(2)}=\sum_{r=1}^{9}\alpha_{4r}\frac{A_{9r}}{b^2}\sin\left(\frac{Z_r\pi}{2}\frac{x_1}{b}\right),\quad u_3^{(2)}=\sum_{r=1}^{9}\alpha_{5r}\frac{A_{9r}}{b^2}\sin\left(\frac{Z_r\pi}{2}\frac{x_1}{b}\right),\quad u_1^{(3)}=\sum_{r=1}^{9}\alpha_{6r}\frac{A_{9r}}{b^3}\cos\left(\frac{Z_r\pi}{2}\frac{x_1}{b}\right),$$

$$u_2^{(4)}=\sum_{r=1}^{9}\alpha_{7r}\frac{A_{9r}}{b^4}\sin\left(\frac{Z_r\pi}{2}\frac{x_1}{b}\right),\quad u_3^{(4)}=\sum_{r=1}^{9}\alpha_{8r}\frac{A_{9r}}{b^4}\sin\left(\frac{Z_r\pi}{2}\frac{x_1}{b}\right),\quad u_1^{(5)}=\sum_{r=1}^{9}\alpha_{9r}\frac{A_{9r}}{b^5}\cos\left(\frac{Z_r\pi}{2}\frac{x_1}{b}\right),$$

where

$$Z_r=\frac{\xi_r}{\frac{\pi}{2b}},\ \alpha_{ir}=\frac{A_{ir}}{A_{9r}},\ i,r=1,2,3,4,5,6,7,8,9.$$

Frequency spectra

As a result, stress components can also be expressed with wavenumber solutions and amplitude ratios. To obtain frequency solutions, we need to utilize the *traction-free boundary conditions*

$$T_5^{(0)} = T_6^{(0)} = T_5^{(2)} = T_6^{(2)} = T_5^{(4)} = T_6^{(4)} = 0$$

$$T_1^{(1)} = T_1^{(3)} = T_1^{(5)} = 0$$

This results in a frequency equation through setting the coefficient matrix of the boundary condition equations to vanish. The frequency spectra in the vicinity of the fifth-order thickness-shear overtone vibrations are given in Fig. 3.

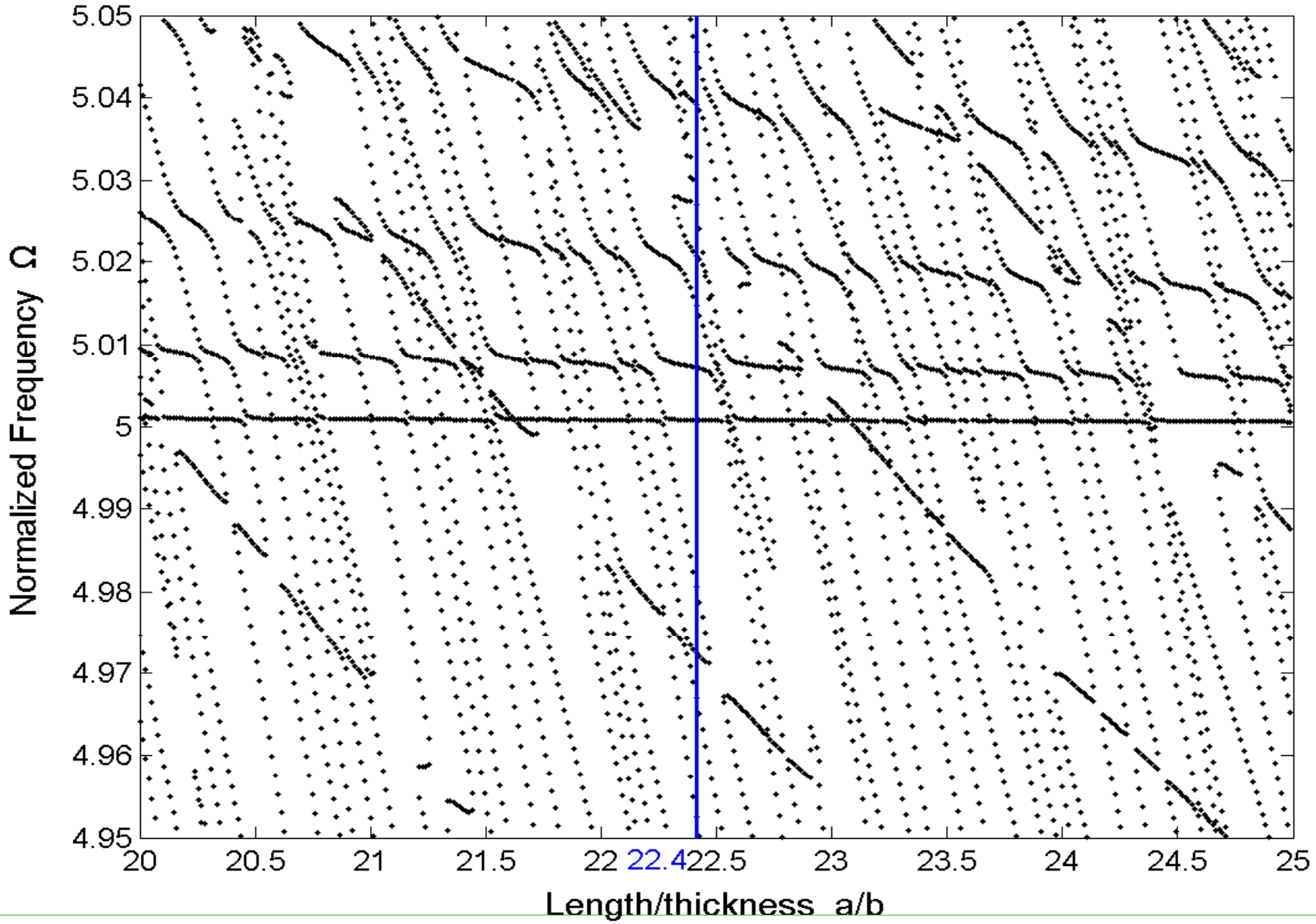


Fig. 3 Frequency spectra of an AT-cut quartz plate vibrating in the vicinity of the fifth-order thickness-shear overtone mode.

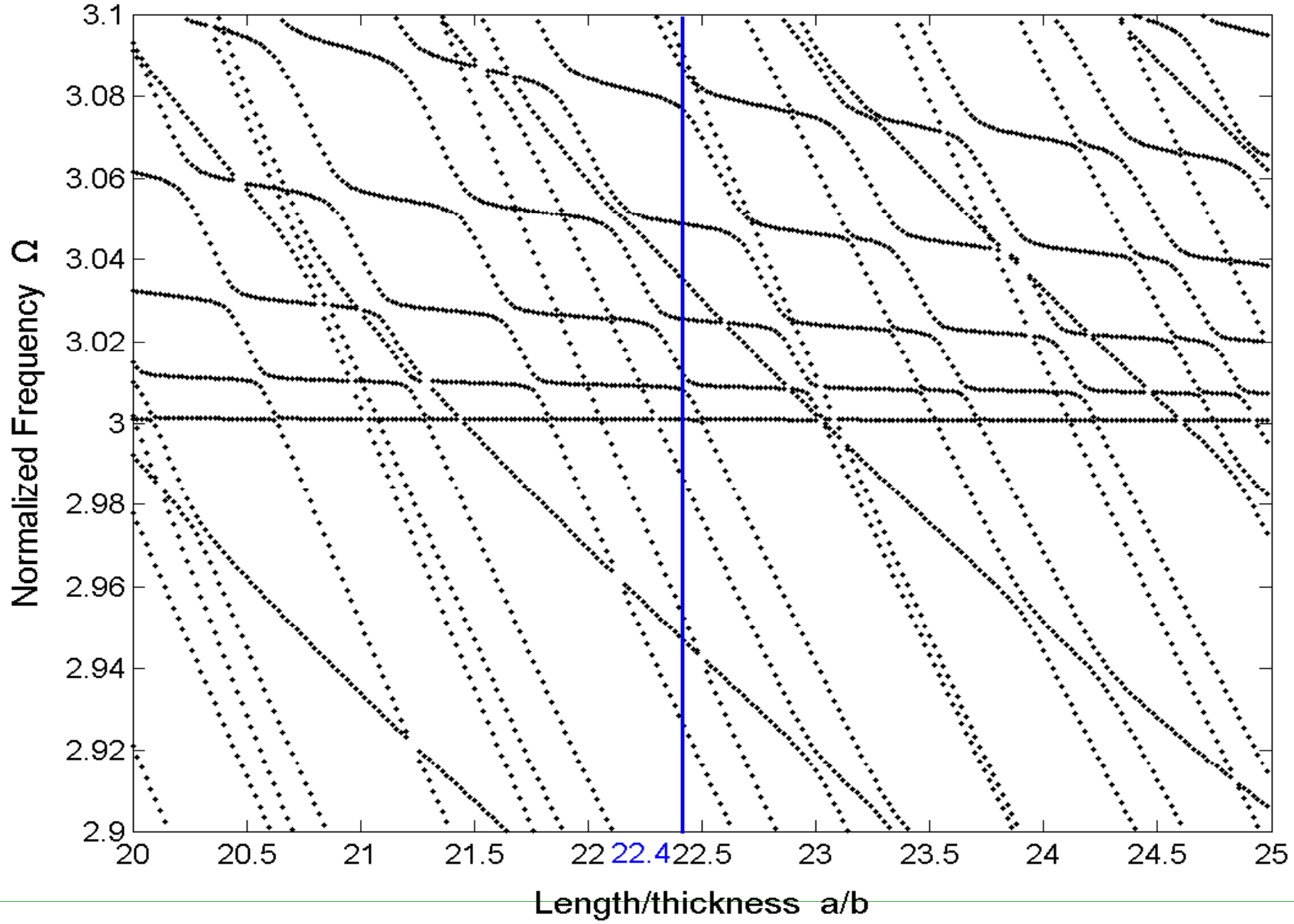


Fig. 4 Frequency spectra of an AT-cut quartz plate vibrating in the vicinity of the third-order thickness-shear overtone mode .

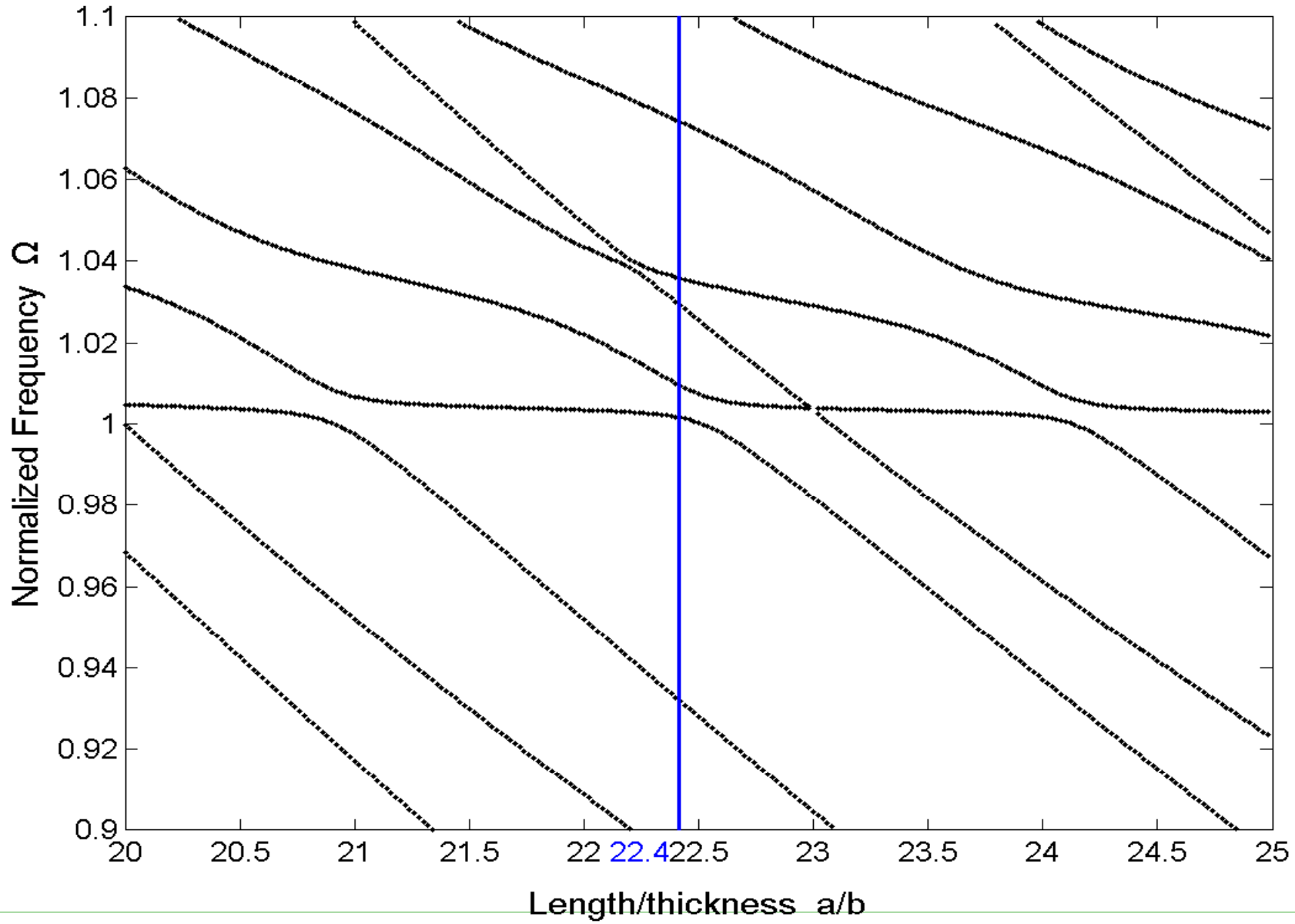


Fig. 5 Frequency spectra of an AT-cut quartz plate vibrating in the vicinity of the fundamental thickness-shear mode .

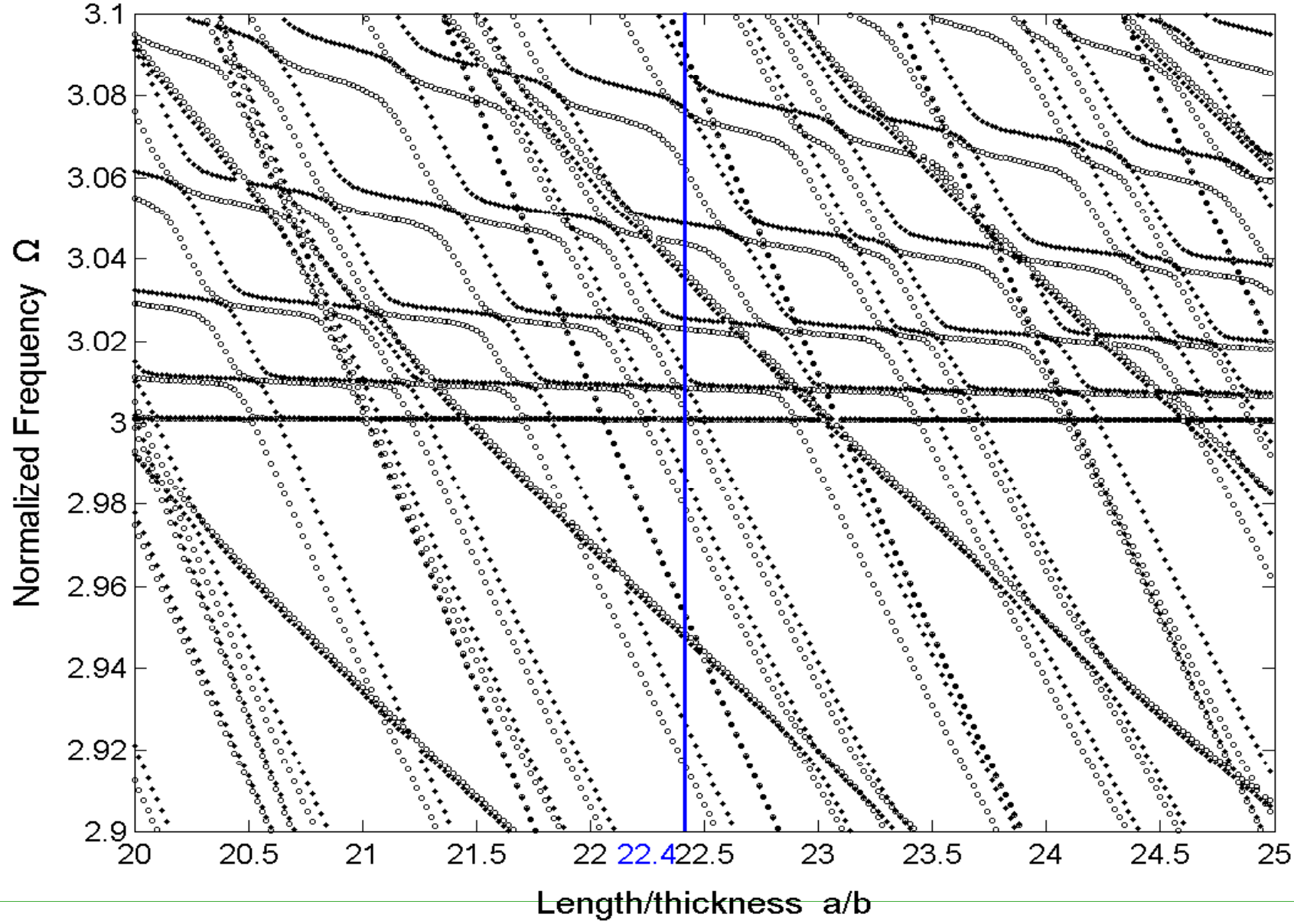


Fig. 6 Comparison of frequency spectra of an AT-cut quartz plate vibrating in the vicinity of the third-order thickness-shear overtone mode .

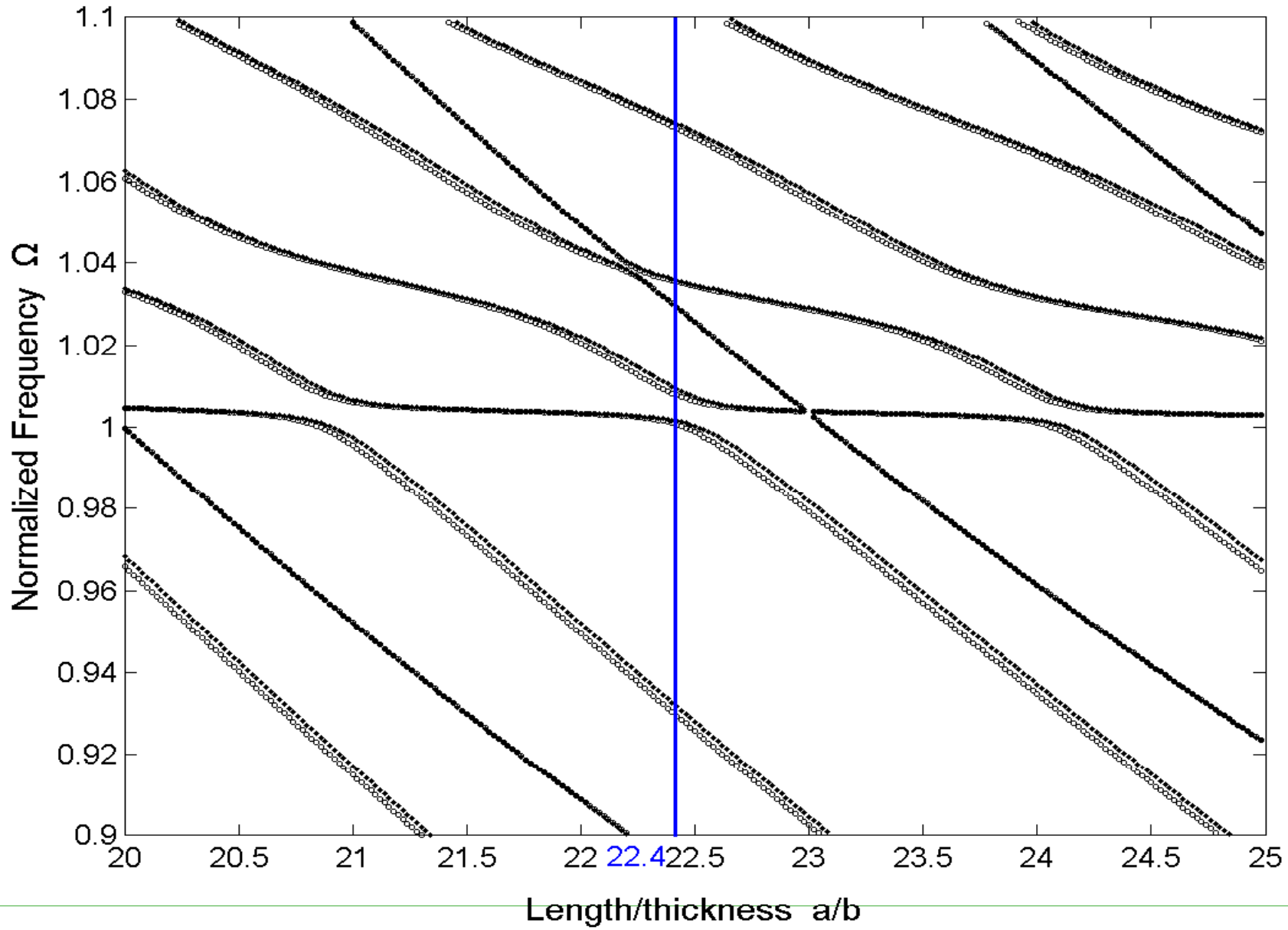


Fig. 7 Comparison of frequency spectra of an AT-cut quartz plate vibrating in the vicinity of the fundamental thickness-shear mode .

Vibration mode shapes

Eventually the displacements are given as

$$u_2^{(0)} = A_{99}\left[\sum_{r=1}^{9}\beta_r\alpha_{1r}\sin\left(\frac{Z_r\pi}{2}\frac{x_1}{b}\right)\right],\ u_3^{(0)} = A_{99}\left[\sum_{r=1}^{9}\beta_r\alpha_{2r}\sin\left(\frac{Z_r\pi}{2}\frac{x_1}{b}\right)\right],\ u_1^{(1)} = \frac{A_{99}}{b}\left[\sum_{r=1}^{9}\beta_r\alpha_{3r}\cos\left(\frac{Z_r\pi}{2}\frac{x_1}{b}\right)\right],$$

$$u_2^{(2)} = \frac{A_{99}}{b^2}\left[\sum_{r=1}^{9}\beta_r\alpha_{4r}\sin\left(\frac{Z_r\pi}{2}\frac{x_1}{b}\right)\right], u_3^{(2)} = \frac{A_{99}}{b^2}\left[\sum_{r=1}^{9}\beta_r\alpha_{5r}\sin\left(\frac{Z_r\pi}{2}\frac{x_1}{b}\right)\right], u_1^{(3)} = \frac{A_{99}}{b^3}\left[\sum_{r=1}^{9}\beta_r\alpha_{6r}\cos\left(\frac{Z_r\pi}{2}\frac{x_1}{b}\right)\right],$$

$$u_2^{(4)} = \frac{A_{99}}{b^4}\left[\sum_{r=1}^{9}\beta_r\alpha_{7r}\sin\left(\frac{Z_r\pi}{2}\frac{x_1}{b}\right)\right], u_3^{(4)} = \frac{A_{99}}{b^4}\left[\sum_{r=1}^{9}\beta_r\alpha_{8r}\sin\left(\frac{Z_r\pi}{2}\frac{x_1}{b}\right)\right], u_1^{(5)} = \frac{A_{99}}{b^5}\left[\sum_{r=1}^{9}\beta_r\alpha_{9r}\cos\left(\frac{Z_r\pi}{2}\frac{x_1}{b}\right)\right],$$

where

$$\beta_i = \frac{A_{9i}}{A_{99}}, i = 1,2,3,4,5,6,7,8,9.$$

Vibration mode shapes

The displacement mode shapes at resonances of predominantly fundamental thickness-shear vibrations, third-order vibrations and fifth-order vibrations are plotted for length to thickness ratio $a/b = 22.4$ as shown in the following figures.

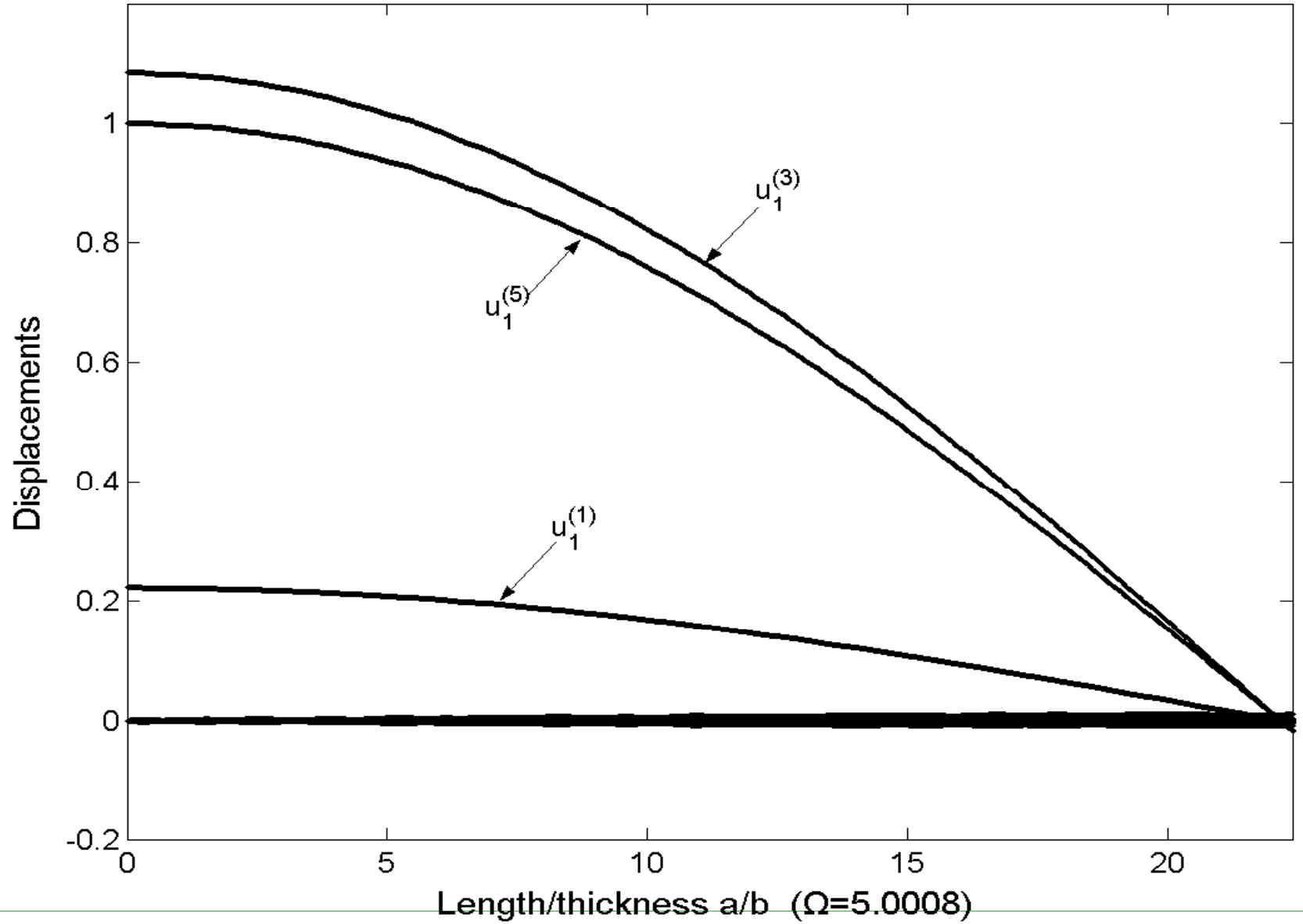


Fig. 8 Displacement amplitudes of all the vibration modes at the fifth-order thickness-shear mode with $a/b = 22.4$ and $\Omega = 5.0008$.

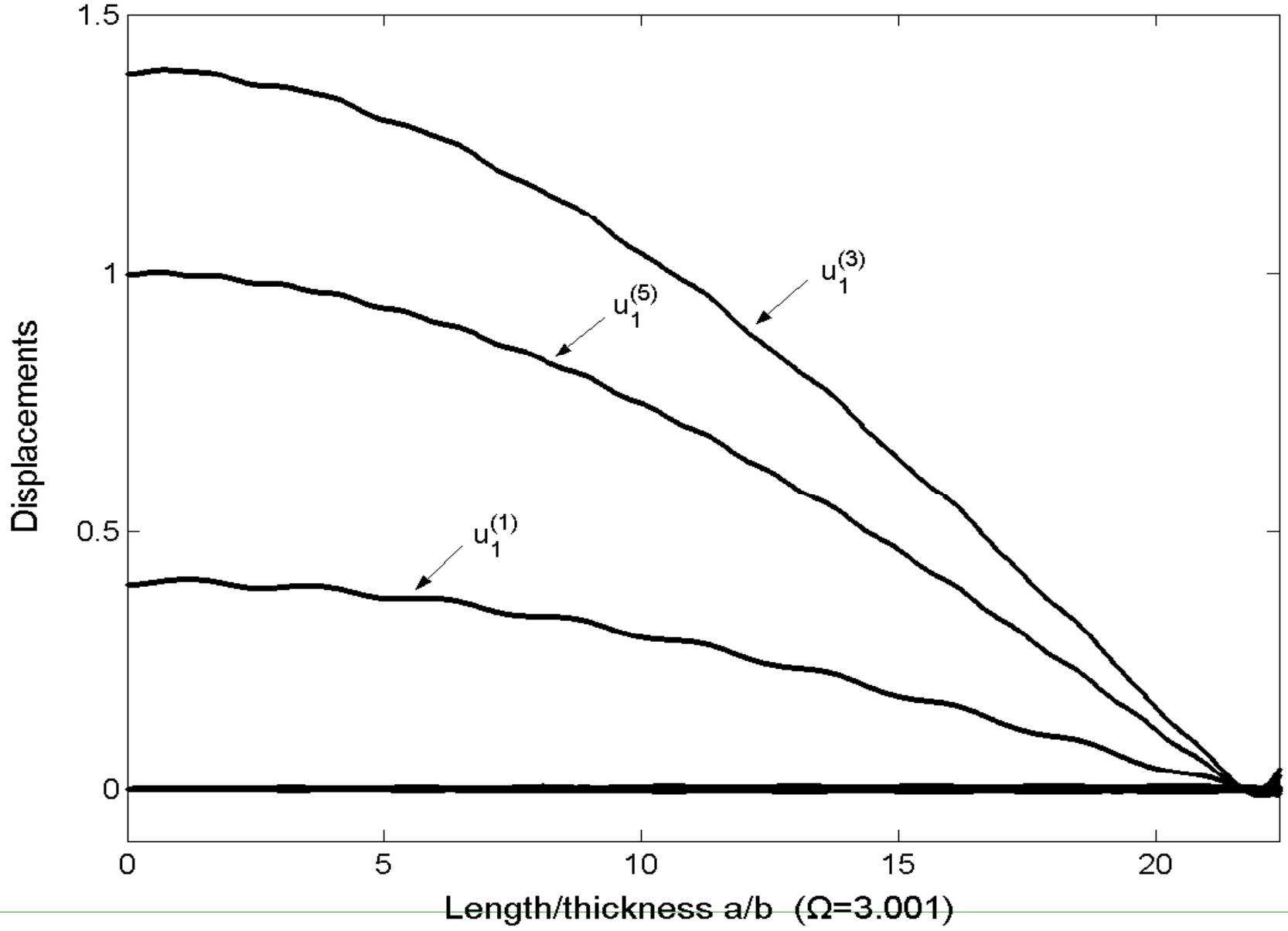


Fig. 9 Displacement amplitudes of all the vibration modes at the third-order thickness-shear mode with $a/b = 22.4$ and $\Omega = 3.001$.

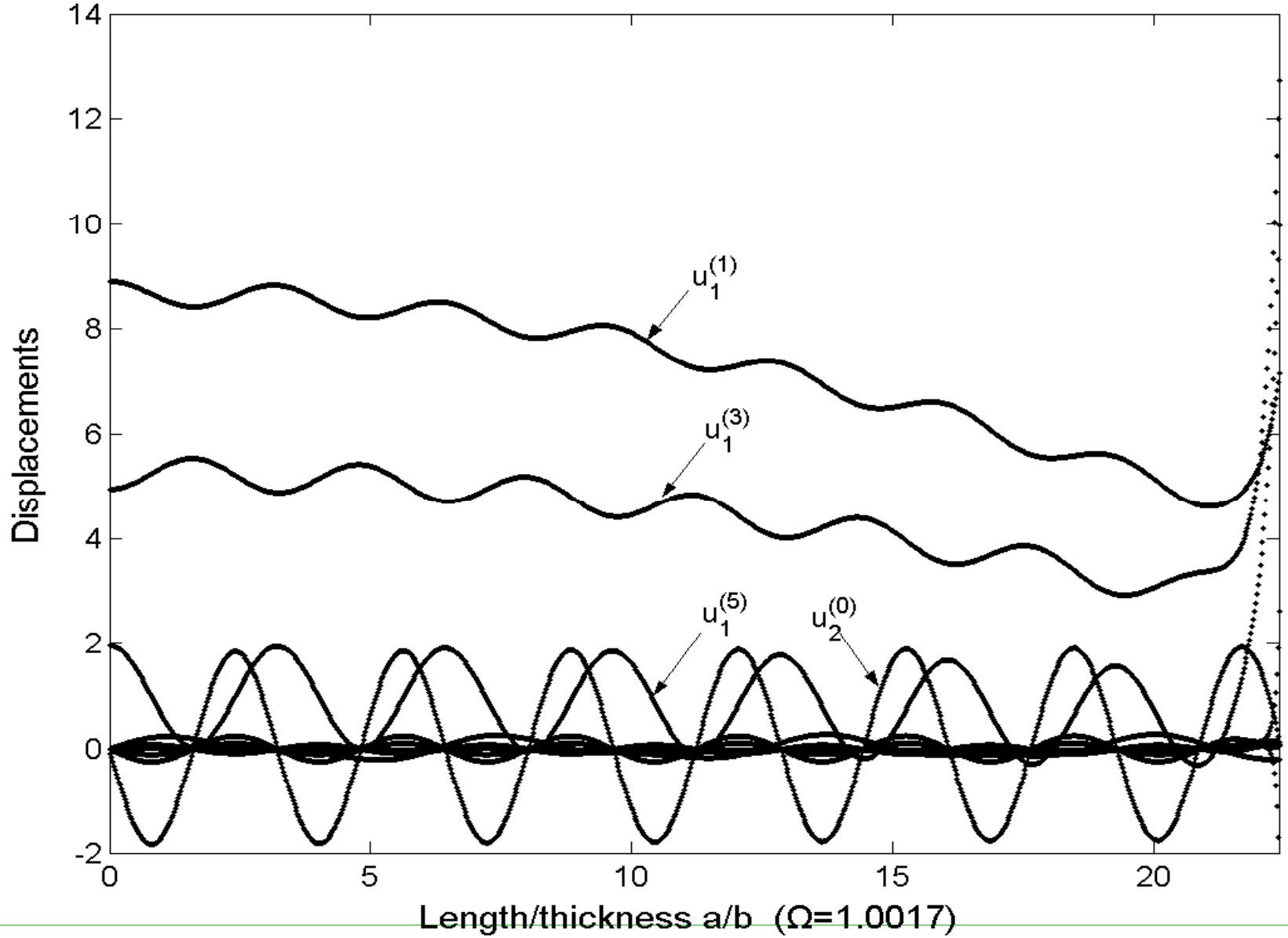


Fig. 10 Displacement amplitudes of all the vibration modes at the fundamental thickness-shear mode with $a/b = 22.4$ and $\Omega = 1.0017$.

Summary

- Mindlin plate equations can be used for the fundamental and overtone mode vibrations of quartz crystal resonators of thickness-shear types.
- Our examples are given with *AT-cut* quartz crystal plates, but the corrected equations can also be used for the vibrations of *SC-cut* quartz crystal plates.
- More accurate and practical analysis of quartz crystal resonators can be done with the corrected Mindlin plate equations for the *finite element analysis*.

提纲

1. 石英晶体谐振器的历史和趋势
2. 弹性波基础
3. 石英晶体
4. 无限大板的厚度振动
5. Mindlin板方程
6. 复杂因素

Temperature Effect

We all know that quartz crystal resonators are sensitive to temperature change, and frequency-temperature relation is one of the important properties in applications. The thermal effect is a typical nonlinear problem with the origin traced to the thermal properties of quartz crystal. Consequently, the study of thermal effect requires the availability of higher-order elastic constants dependence on the temperature to predict the known cubic feature of the thickness-shear vibration frequency. Apparently, as plate theories have been widely adopted for their natural appealing and usefulness in the analysis of quartz crystal resonators with plates as the core element, the consideration of thermal effect in the framework of the Mindlin plate theory has been presented and utilized. In particular, the finite element implementation of the Mindlin plate equations with the consideration of thermal fields has been successful in the prediction of the frequency-temperature relations.

Temperature Effect-continued

The equations of motion of a piezoelectric plate based on the incremental theory is (Lee, P.C.Y., Yong, Y.-K.: Frequency–temperature behavior of thickness vibrations of doubly rotated quartz plates affected by plate dimensions and orientations. *J. Appl. Phys.* 60, 2327–2341, 1986)

$$\beta_{ik} t_{kj,j}^{(n)} - n\beta_{ik} t_{k2}^{(n-1)} + \beta_{ik} F_k^{(n)} = \rho \sum_{m=0}^{\infty} B_{mn} \ddot{u}_i^{(m)}, i, j, k = 1,2,3,$$

where the linear thermal expansion coefficients

$$\beta_{ik} = \delta_{ik} + \alpha_{ik}^{\theta},$$
$$\alpha_{ik}^{\theta} = \alpha_{ik}^{(1)} \Theta + \alpha_{ik}^{(2)} \Theta^2 + \alpha_{ik}^{(3)} \Theta^3,$$

Temperature Effect-continued

Constitutive relation is

$$t_{ij}^{(n)} = \sum_{m=0}^{\infty} B_{mn} D_{ijkl} e_{kl}^{(m)},$$

$$e_{kj}^{(n)} = \frac{1}{2}\left[\beta_{ik} u_{i,k}^{(n)} + \beta_{ik} u_{i,j}^{(n)} + (n+1)\left(\delta_{2k}\beta_{ij} u_i^{(n+1)} + \delta_{2j}\beta_{ik} u_i^{(n+1)}\right)\right],$$

where thermal elastic constants $D_{ijkl}\,(i,j,k,l = 1,2,3)$ are

$$D_{ijkl} = c_{ijkl} + d_{ijkl}^{(1)}\Theta + d_{ijkl}^{(2)}\Theta^2 + d_{ijkl}^{(3)}\Theta^3, \Theta = T - 25℃.$$

Temperature Effect-continued

Table Thermal expansion coefficients of quartz crystal

ij	$\alpha_{ij}^{(1)}, 10^{-6}$ /℃	$\alpha_{ij}^{(2)}, 10^{-9}$ /℃^{2}	$\alpha_{ij}^{(3)}, 10^{-12}$ /℃^{3}
11	13.71	6.5	-1.9
22	13.71	6.5	-1.9
33	7.47	2.9	-1.5

Sources:

R. Bechmann, A. D. Ballato, and T. J. Lukaszek, Higher order temperature coefficients of the elastic stiffnesses and compliances of Alpha-quartz", *Proc. of the IRE*, **50** (8), 1812-1822, 1962.

Yook-Kong Yong and Shigeo Kanna, IDT geometry and crystal cut effects on the frequency-temperature curves of a SAW periodic structure of quartz, *Proc. of the 1998 IEEE International Ultrasonics Symposium*, 223-228.

Temperature Effect-continued

$$D_{pq}^{(1)} = \begin{bmatrix} -0.592169 & -1.65828 & -1.03537 & 0.427555 & & \\ & -1.63965 & -0.158273 & -0.651106 & & \\ & & -2.43330 & -0.0175359 & & \\ & & & -0.396439 & & \\ & & & & -0.366579 & -0.855763 \\ & & & & & -0.0805899 \end{bmatrix} \times 10^7\ \mathrm{N/^{\circ}C \cdot m^2},$$

$$D_{pq}^{(2)} = \begin{bmatrix} -1.01190 & -1.79202 & -1.64226 & 0.503413 & & \\ & -2.70317 & 0.155307 & -0.613946 & & \\ & & -2.74640 & 0.260943 & & \\ & & & -0.204786 & & \\ & & & & -0.943378 & -0.994985 \\ & & & & & -0.0319257 \end{bmatrix} \times 10^4\ \mathrm{N/^{\circ}C^2 \cdot m^2},$$

$$D_{pq}^{(3)} = \begin{bmatrix} -0.537020 & 2.27503 & -0.955304 & -0.182843 & & \\ & -2.22281 & 0.769925 & 0.559134 & & \\ & & 1.04705 & -0.320487 & & \\ & & & 0.557183 & & \\ & & & & -1.87182 & 0.812975 \\ & & & & & 0.653236 \end{bmatrix} \times 10^1\ \mathrm{N/^{\circ}C^3 \cdot m^2},$$

Temperature Effect-continued

First-order equations (P C Y Lee and Ji Wang, Frequency–temperature relations of thickness-shear and flexural vibrations of contoured quartz resonators, *J. Appl. Phys.* **80** (6), 3457-3465, 1996,)

First of all, the thermal parameters for Y-cut of quartz crystals are the following:

$\beta_1 = \beta_{11}, \beta_2 = \beta_{22}, \beta_3 = \beta_{33}, \beta_4 = \beta_{23}, \beta_{12} = \beta_{13} = 0.$

The first-order equations of motion:

$$\beta_1\left(t_{1,1}^{(0)} + t_{5,3}^{(0)}\right) + \beta_1 F_1^{(0)} = 2b\rho\ddot{u}_1^{(0)},$$

$$\beta_2\left(t_{6,1}^{(0)} + t_{4,3}^{(0)}\right) + \beta_4\left(t_{5,1}^{(0)} + t_{3,3}^{(0)}\right) + \beta_2 F_2^{(0)} + \beta_4 F_3^{(0)} = 2b\rho\ddot{u}_2^{(0)},$$

$$\beta_4\left(t_{6,1}^{(0)} + t_{4,3}^{(0)}\right) + \beta_3\left(t_{5,1}^{(0)} + t_{3,3}^{(0)}\right) + \beta_4 F_2^{(0)} + \beta_3 F_3^{(0)} = 2b\rho\ddot{u}_3^{(0)},$$

$$\beta_1\left(t_{1,1}^{(1)} + t_{5,3}^{(1)}\right) - \beta_1 t_6^{(0)} + \beta_1 F_1^{(0)} = \frac{2b^3}{3}\rho\ddot{u}_1^{(1)},$$

$$\beta_2\left(t_{6,1}^{(1)} + t_{4,3}^{(1)}\right) + \beta_4\left(t_{5,1}^{(1)} + t_{3,3}^{(1)}\right) - \beta_2 t_2^{(0)} - \beta_4 t_4^{(0)} + \beta_2 F_2^{(1)} + \beta_4 F_3^{(1)} = \frac{2b^3}{3}\rho\ddot{u}_2^{(1)},$$

$$\beta_4\left(t_{6,1}^{(1)} + t_{4,3}^{(1)}\right) + \beta_3\left(t_{5,1}^{(1)} + t_{3,3}^{(1)}\right) - \beta_4 t_2^{(0)} - \beta_3 t_4^{(0)} + \beta_4 F_2^{(1)} + \beta_3 F_3^{(1)} = \frac{2b^3}{3}\rho\ddot{u}_3^{(1)},$$

Temperature Effect-continued

$$t_1^{(0)} = 2b\left[D_{11}\beta_1 u_{1,1}^{(0)} + (D_{13}\beta_4 + \kappa D_{14}\beta_2)u_{2,3}^{(0)} + (D_{13}\beta_3 + \kappa D_{14}\beta_4)u_{3,3}^{(0)} + \kappa(D_{12}\beta_2 + D_{14}\beta_4)u_2^{(1)} + \kappa(D_{12}\beta_4 + D_{14}\beta_3)u_3^{(1)}\right],$$

$$t_2^{(0)} = 2b\left[D_{21}\beta_1 u_{1,1}^{(0)} + (D_{23}\beta_4 + \kappa D_{24}\beta_2)u_{2,3}^{(0)} + (D_{23}\beta_3 + \kappa D_{24}\beta_4)u_{3,3}^{(0)} + \kappa(D_{22}\beta_2 + D_{24}\beta_4)u_2^{(1)} + \kappa(D_{22}\beta_4 + D_{24}\beta_3)u_3^{(1)}\right],$$

$$t_3^{(0)} = 2b\left[D_{21}\beta_1 u_{1,1}^{(0)} + (D_{23}\beta_4 + \kappa D_{24}\beta_2)u_{2,3}^{(0)} + (D_{23}\beta_3 + \kappa D_{24}\beta_4)u_{3,3}^{(0)} + \kappa(D_{32}\beta_2 + D_{34}\beta_4)u_2^{(1)} + \kappa(D_{32}\beta_4 + D_{34}\beta_3)u_3^{(1)}\right],$$

$$t_4^{(0)} = 2b\left[D_{21}\beta_1 u_{1,1}^{(0)} + (D_{23}\beta_4 + \kappa D_{24}\beta_2)u_{2,3}^{(0)} + (D_{23}\beta_3 + \kappa D_{24}\beta_4)u_{3,3}^{(0)} + \kappa(D_{42}\beta_2 + D_{44}\beta_4)u_2^{(1)} + \kappa(D_{42}\beta_4 + D_{44}\beta_3)u_3^{(1)}\right],$$

$$t_5^{(0)} = 2b\left[D_{55}\beta_1 u_{1,3}^{(0)} + (D_{55}\beta_4 + \kappa D_{56}\beta_2)u_{2,1}^{(0)} + (D_{55}\beta_3 + \kappa D_{56}\beta_4)u_{3,1}^{(0)} + \kappa D_{56}\beta_1 u_1^{(1)}\right],$$

$$t_6^{(0)} = 2b\left[D_{65}\beta_1 u_{1,3}^{(0)} + (D_{65}\beta_4 + \kappa D_{66}\beta_2)u_{2,1}^{(0)} + (D_{65}\beta_4 + \kappa D_{66}\beta_2)u_{3,1}^{(0)} + \kappa D_{66}\beta_1 u_1^{(1)}\right];$$

$$t_1^{(1)} = \frac{2b^3}{3}\left[\bar{D}_{11}\beta_1 u_{1,1}^{(1)} + (\bar{D}_{13}\beta_4 + \bar{D}_{14}\beta_2)u_{2,3}^{(1)} + (\bar{D}_{13}\beta_3 + \bar{D}_{14}\beta_4)u_{3,3}^{(1)}\right],$$

$$t_2^{(1)} = \frac{2b^3}{3}\left[\bar{D}_{21}\beta_1 u_{1,1}^{(1)} + (\bar{D}_{23}\beta_4 + \bar{D}_{24}\beta_2)u_{2,3}^{(1)} + (\bar{D}_{23}\beta_3 + \bar{D}_{24}\beta_4)u_{3,3}^{(1)}\right],$$

$$t_3^{(1)} = \frac{2b^3}{3}\left[\bar{D}_{31}\beta_1 u_{1,1}^{(1)} + (\bar{D}_{33}\beta_4 + \bar{D}_{34}\beta_2)u_{2,3}^{(1)} + (\bar{D}_{33}\beta_3 + \bar{D}_{34}\beta_4)u_{3,3}^{(1)}\right],$$

$$t_4^{(1)} = \frac{2b^3}{3}\left[\bar{D}_{41}\beta_1 u_{1,1}^{(1)} + (\bar{D}_{43}\beta_4 + \bar{D}_{44}\beta_2)u_{2,3}^{(1)} + (\bar{D}_{43}\beta_3 + \bar{D}_{44}\beta_4)u_{3,3}^{(1)}\right],$$

$$t_5^{(1)} = \frac{2b^3}{3}\left[\bar{D}_{55}\beta_1 u_{1,3}^{(1)} + (\bar{D}_{55}\beta_4 + \bar{D}_{56}\beta_2)u_{2,3}^{(1)} + (\bar{D}_{55}\beta_3 + \bar{D}_{56}\beta_4)u_{3,1}^{(1)}\right],$$

$$t_6^{(1)} = \frac{2b^3}{3}\left[\bar{D}_{65}\beta_1 u_{1,3}^{(1)} + (\bar{D}_{65}\beta_4 + \bar{D}_{66}\beta_2)u_{2,3}^{(1)} + (\bar{D}_{65}\beta_3 + \bar{D}_{66}\beta_4)u_{3,1}^{(1)}\right];$$

$$\kappa^2 = \frac{\pi^2}{12}, \bar{D}_{ij} = D_{ij} - \frac{D_{i2}\beta_2 + D_{i4}\beta_4}{D_{22}\beta_2 + D_{24}\beta_4}D_{2j}, i, j = 1, 3, 4.$$

Temperature Effect-continued

Strain-displacement relations

$$e_1^{(0)} = \beta_1 u_{1,1}^{(0)},$$
$$e_2^{(0)} = \beta_2 u_2^{(1)} + \beta_4 u_3^{(1)},$$
$$e_3^{(0)} = \beta_4 u_{2,3}^{(0)} + \beta_3 u_{3,3}^{(0)},$$
$$e_4^{(0)} = \beta_2 u_{2,3}^{(0)} + \beta_4 u_{3,3}^{(0)} + \beta_4 u_2^{(1)} + \beta_3 u_3^{(1)},$$
$$e_5^{(0)} = \beta_1 u_{1,3}^{(0)} + \beta_4 u_{2,1}^{(0)} + \beta_3 u_{3,1}^{(0)},$$
$$e_6^{(0)} = \beta_2 u_{2,1}^{(0)} + \beta_4 u_{3,1}^{(0)} + \beta_1 u_1^{(1)};$$
$$e_1^{(1)} = \beta_1 u_{1,1}^{(1)},$$
$$e_2^{(1)} = 2\beta_2 u_2^{(2)},$$
$$e_3^{(1)} = \beta_4 u_{2,3}^{(1)} + \beta_3 u_{3,3}^{(1)},$$
$$e_4^{(1)} = \beta_2 u_{2,3}^{(1)} + \beta_4 u_{3,3}^{(1)},$$
$$e_5^{(1)} = \beta_1 u_{1,3}^{(1)} + \beta_4 u_{2,1}^{(1)} + \beta_3 u_{3,1}^{(1)},$$
$$e_6^{(0)} = \beta_2 u_{2,1}^{(1)} + \beta_4 u_{3,1}^{(1)},$$
$$2u_2^{(2)} = -\frac{1}{D_{22}\beta_2 + D_{24}\beta_4}\left[D_{21}\beta_1 u_{1,1}^{(1)} + (D_{23}\beta_4 + D_{24}\beta_2)u_{2,3}^{(1)} + (D_{23}\beta_4 + D_{24}\beta_2)u_{3,3}^{(1)}\right].$$

Temperature Effect-continued

For demonstration purpose, the coupled thickness-shear and flexural vibrations under temperature variation are

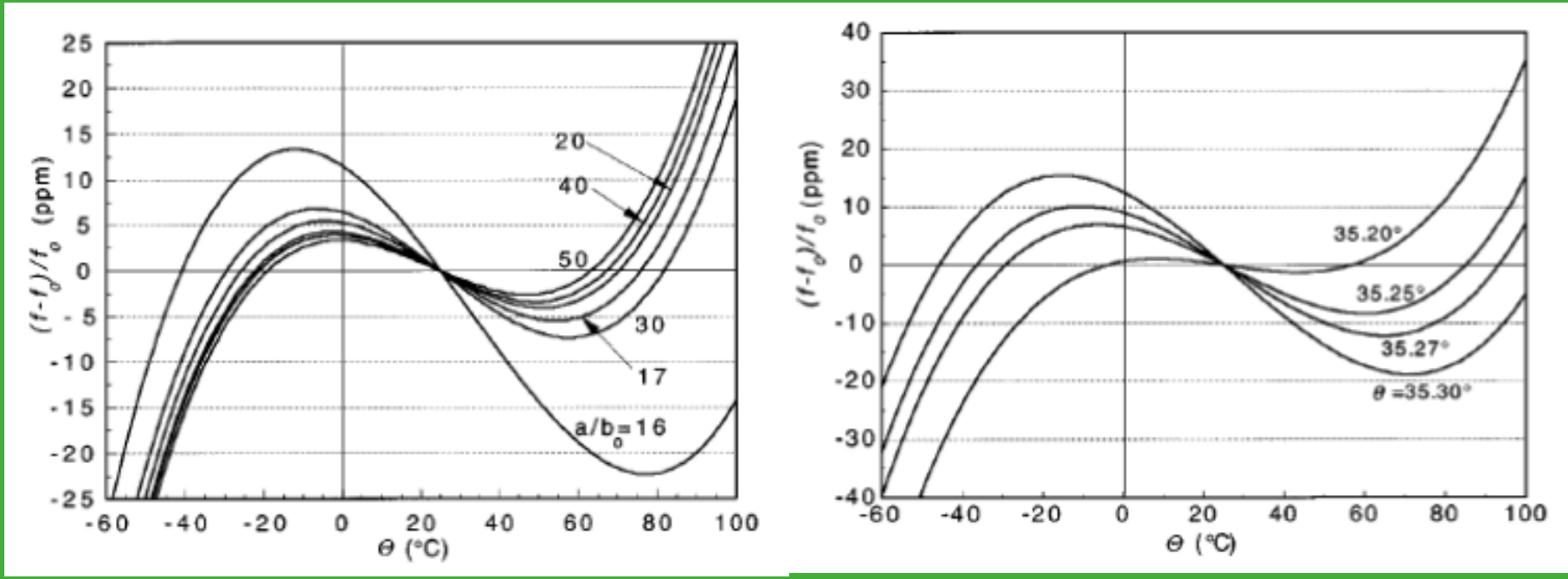
$$\beta_2 t_{6,1}^{(0)} + \beta_2 F_2^{(0)} = 2b\rho\ddot{u}_2^{(0)},$$

$$\beta_1 t_{1,1}^{(1)} - \beta_1 t_6^{(0)} + \beta_1 F_1^{(1)} = \frac{2b^3}{3}\rho\ddot{u}_1^{(1)},$$

$$t_6^{(0)} = 2\kappa^2 b D_{66}\left(\beta_2 u_{2,1}^{(0)} + \beta_1 u_1^{(1)}\right),$$

$$t_1^{(1)} = \frac{2b^3}{3}\tilde{D}_{11}\beta_1 u_{1,1}^{(1)}.$$

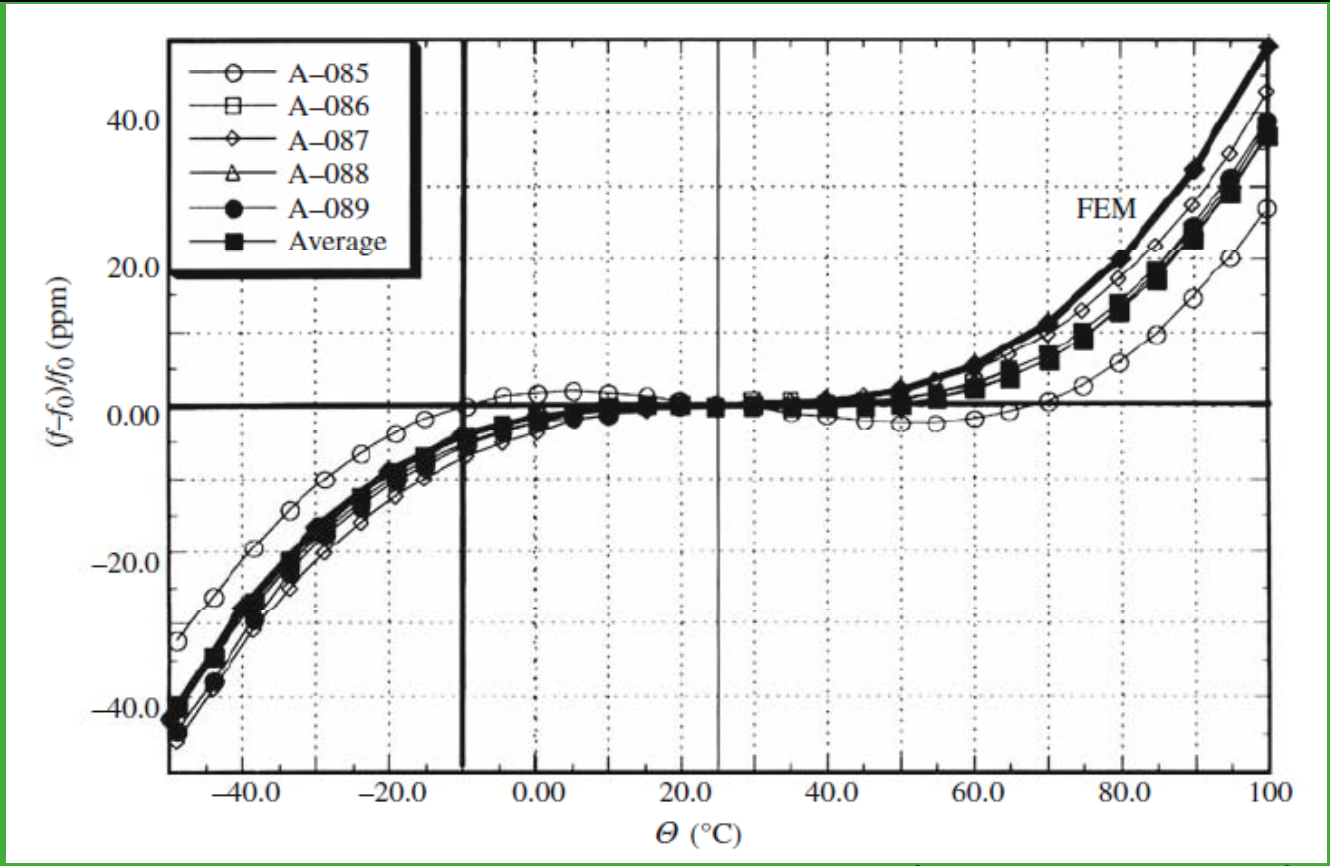
Temperature Effect-continued



Effects of quartz crystal blank parameters on the frequency-temperature relation (a/b_0: electroded region; θ: rotation angle)

P. C. Y. Lee and J. Wang, Frequency–temperature relations of thickness-shear and flexural vibrationsof contoured quartz resonators, *J. Appl. Phys.* **80** (6), 3457-3465,1996.

Temperature Effect-continued



Ji Wang, Jiun-Der Yu, Yook-Kong Yong, and Tsutomu Imai, A finite element analysis of frequency–temperature relations of AT-cut quartz crystal resonators with higher-order Mindlin plate theory, *Acta Mechanica*, **199**(1-4), 117-130, 2008

Electrode Effect

- Electrodes on the faces of quartz crystal plates are essential for the making of resonators, and the roles are beyond the electrical driving of piezoelectric solid.
- One of the important factors of the outstanding performance of quartz crystal resonators, energy trapping, which confines the vibration energy in the region under the electrodes, is also defined by the presence of electrodes which modifies the thicknesses of plate in different regions.
- Referring to the dispersion curves for the fundamental thickness-shear vibration mode, we can clearly observe that the wavenumber solutions are imaginary for frequency below the cut-off value are real above the cut-off frequency.
- With given displacement solutions in trigonometric functions and noting the fact that the frequency of a quartz crystal plate with partial electrodes will be somewhere between the electrode part (less than 1) and the crystal plate (exactly 1), the displacement solutions in the electrode portion will be trigonometric functions to maintain a constant vibrations while in the crystal blank which will be hyperbolic trigonometric functions that quickly diminish at the ends. This means the confinement of thickness-shear vibrations is realized by both electrodes and beveling at least in a typical quartz crystal resonator.

Electrode Effect - continued

For an infinite plate with symmetric electrodes, we have the frequency equation (Bleustein, J.L., Tiersten., H.F., 1968. Forced thickness-shear vibrations of discontinuously plated piezoelectric plates. J. Acoust. Soc. Amer., 43(6):1311-1318; Ji Wang and Li-jun Shen, Exact thickness-shear resonance frequency of electroded piezoelectric crystal plates, J. Zhejiang University Science, 6A (9), 980-985, 2005; Jiashi Yang, Honggang Zhou, and Weiping Zhang: Thickness-Shear Vibration of Rotated Y-cut Quartz Plates with Relatively Thick Electrodes of Unequal Thickness, *IEEE Transactions on Ultrasonics Ferroelectrics and Frequency Control*, 52 (5): 918-922, 2005)

$$\tan\xi\tan\frac{2B}{k}\xi=\frac{k}{C_{66}},$$

with the consideration of piezoelectric effect, the frequency equation will take the form of

$$\xi\tan\xi\tan\frac{2B}{k}\xi=\frac{K}{C_{66}}[(1+k_{26}^2)\xi-k_{26}^2\tan\xi],$$

where the key parameters are

$$k=\frac{\rho}{\bar{\rho}}C_{66},C_{66}=\frac{\bar{c}_{66}}{c_{66}},B=\frac{\bar{b}}{b},K^2=\frac{k^2}{1+k_{26}^2},k_{26}^2=\frac{e_{26}^2}{c_{66}\epsilon_{22}}.$$

The accurate solutions of the thickness-shear vibration frequency are important in the validation of plate theory and precise design of resonators.

Electrode Effect – continued

Relatively Thicker Electrodes with Mindlin Plate Theory (Ji Wang, Consideration of stiffness and mass effects of relatively thicker electrodes with Mindlin plate theory, *IEEE Transactions on Ultrasonics, Ferroelectrics, and Frequency Control*, **53** (6), 1218-1221, 2006)

$$\rho_m^{(n)} = \rho\left[1 + (m+n+1)\frac{2\bar{\rho}\bar{b}}{\rho b}\right] = \rho[1 + (m+n+1)R],$$

$$c_{ijkl}^{(m,n)} = c_{ijkl}\left[1 + (m+n+1)\frac{2\bar{c}_{ijkl}\,\bar{b}}{c_{ijkl}\,b}\right],$$

where $R = (2\bar{\rho}\bar{b})/\rho b$ is known as mass ratio. The plate equations with the density and stiffness of electrodes considered can be obtained by replacing ρ and c_{ijkl} with the newer definitions in the two-dimensional expressions. These equations will be capable to consider the effect of the electrodes.

Our experiences indicate that for thin electrodes the mass effect will be enough. But as the resonators shrink in their sizes, the electrodes will be more important and the validation of the mass and stiffness consideration will be important.

Electrode Effect – continued

One important result which is familiar to us is the principle for the determination of electrode size with the Bechmann's number, which specifies the minimum and optimal lengths of electrodes based on the energy trapping consideration. The essential argument is that for the resonator to have better property, it should trap the inharmonic modes under the electrode. It will be better if the only one mode is trapped with a minimum electrode. The Bechmann's number is first presented as an empirical observation, but later efforts have been successfully proven that such a parameter does exist and can be obtained analytically. The derivation here is from Mindlin (R. D. Mindlin, Bechmann's number for harmonic overtones of thickness/twist vibrations of rotated-Y-cut quartz plates, *Journal of the Acoustical Society of America*, 41 (4, Part 2): 969-973, 1967).

Electrode Effect – continued

For a plate with thickness/twist vibrations, we assume

$u_1 = U(x_2, x_3)e^{i\omega t}, u_2 = u_3 = 0,$

and consequently we have strain components as

$S_1 = S_2 = S_3 = S_4 = 0,$

$S_5 = \frac{\partial U}{\partial x_3}, S_6 = \frac{\partial U}{\partial x_2}.$

The stress components for monolithic crystals are

$T_1 = T_2 = T_3 = T_4 = 0,$

$T_5 = c_{55}\frac{\partial U}{\partial x_3} + c_{56}\frac{\partial U}{\partial x_2},$

$T_6 = c_{65}\frac{\partial U}{\partial x_3} + c_{66}\frac{\partial U}{\partial x_2},$

and the equation of motion will be reduced to

$$c_{66}\frac{\partial^2 U}{\partial x_2^2} + 2c_{56}\frac{\partial^2 U}{\partial x_2 x_3} + c_{66}\frac{\partial^2 U}{\partial x_3^2} = -\omega^2 \rho U.$$

Electrode Effect – continued

The proper thickness-twist displacement for the above equation will be

$$U = A\sin\eta x_2 \cos\zeta\left(\frac{c_{56}}{c_{66}}x_2 - x_3\right),$$

and the substitution into the equations of motion will give

$$\omega^2\rho = c_{66}\eta^2 + \left(c_{55} - \frac{c_{56}^2}{c_{66}}\right)\zeta^2.$$

With traction-free boundary conditions

$$\omega^2 = \frac{c_{66}}{\rho}\left(\frac{\pi}{2h}\right)^2\left[m^2 + \frac{\gamma_{55}}{c_{66}}\left(\frac{2\zeta h}{\pi}\right)^2\right],$$

For electroded plate, we have

$$\bar{\zeta}h = \frac{\pi}{2}\sqrt{\frac{c_{66}}{\gamma_{55}}\left[\bar{\Omega}^2 - \left(\frac{2\bar{\eta}h}{\pi}\right)^2\right]}.$$

Eventually, after algebraic manipulations, the Bechmann's number is

$$\frac{2w}{2h} \le B_{TT} = \frac{1}{m\sqrt{R}}\sqrt{\frac{2\gamma_{55}}{c_{66}}},$$

where R is the mass ratio and m is the order of the overtone. For AT-cut of quartz, we have

$$B_{TT} = \frac{2.17}{m\sqrt{R}}.$$

The empirical numbers are

$$B_{TT} = \frac{M(m)}{m\sqrt{R}}, M(1) = 1.41, M(2) = 2.83, M\ (3) = 4.24, M\ (4) = 5.66.$$

Electrode Effect – continued

The optimal electrode length for AT-cut of quartz crystal at the fundamental thickness-shear modes in x_1 direction has been given by Mindlin and Lee (R. D. Mindlin and P. C. Y. Lee, Thickness-shear and flexural vibrations of partially plated, crystal plates, *Int. J. Solids Struct.*, 2: 125-139, 1966)

$$\frac{w}{h} = m\pi\sqrt{3 + \frac{\pi^2 c_{66}}{4\gamma_{11}}} \approx 1.6m, \gamma_{11} \approx c_{11}, m = 1,2,3,\cdots.$$

With the consideration of effect of electrodes, optimal length should be

$$\frac{w}{h} = \pi\sqrt{\frac{1}{6} + \frac{4\gamma_{11}}{\pi^2 c_{66}}}\frac{1}{\sqrt{R}} \approx \frac{2.75}{\sqrt{R}}, \gamma_{11} \approx c_{11}.$$

This result has been validated by experimental data of Curran and Koneval (D. R. Curran and D. J. Koneval, Factors in the design of VHF filters, *Proceedings of the 19th Annual Symposium on Frequency Control*, 213-268, 1965).

Electrical Parameters

For the formulation of electrical properties of a quartz crystal resonator, we have to introduce the material viscosity to start. It is generally known that the quality factor of a quartz crystal resonator is the measure of energy loss due to the material and structural viscosity. As a result, for the formulation of electrical properties, we need the viscosity of quartz crystal, which were measured by Lamb and Richter (J. Lamb, J. Richter, Anisotropic acoustic attenuation with new measurements for quartz at room temperatures, *Proc. R. Soc. London* 293A (1966) 479 – 492.).

First, the surface charge is (Ji Wang, Wenhua Zhao, and Jianke Du: The determination of electrical parameters of quartz crystal resonators with the consideration of dissipation, *Ultrasonics*, 44 (S1): 869-873, 2006)

$$Q_s = \int_A D_2 dA,$$

and the electrical current is

$$I = -\dot{Q}_s,$$

As a result, with alternating driving voltage on the faces as $\phi_0 e^{i\omega t}$, we have the impedance

$$Z = \frac{2\phi_0 e^{i\omega t}}{I},$$

which gives the resistance as

$$R = \mathrm{Re}\,(Z).$$

The dynamic capacitance of a resonator is

$$C_m = \frac{Q_s}{2\phi_0 e^{i\omega t}},$$

And the capacitance ratio can be calculated accordingly with the readily available static capacitance.

Finally, the quality factor will be

$$Q = \frac{1}{\omega R C_m} = \frac{1}{\omega \mathrm{Re}(Z) C_m}.$$

Activity Dip

- In the temperature variation process, there will be time intervals that the resonator will stop functioning without a signal output. This is considered as a major defect of quartz crystal resonators, but the occurrence of such a phenomenon, frequently referred to as activity dip, has puzzled engineers for long time and eliminating the activity dip has been a top priority in product development. Detailed analysis of the temperature change and vibration modes coupling revealed that the activity dip actually is caused by the vibration mode conversion due to the changes of coupling of multiple vibration modes in finite plates. Many approximate analyses will not be able to find all the vibration modes in the frequency vicinity, resulting the difficulty of predicting the accurate occurrence of the activity in terms of temperature. The challenge is compounded by the modification of the structure and frequency which are also inconsistent with known nominal properties of resonators.
- The solution to the activity problem is to have accurate analysis of vibration frequency and the effect of structural modifications in terms of electrodes, mounting, packaging, and thermal variation. The design parameters should be selected to be least sensitive to temperature change and the mode conversion should be excluded from the adjacent areas. Obviously, the preliminary step in making activity dip free design is to have accurate frequency spectra, or the frequency dependence on the structural parameters, in the product development process.

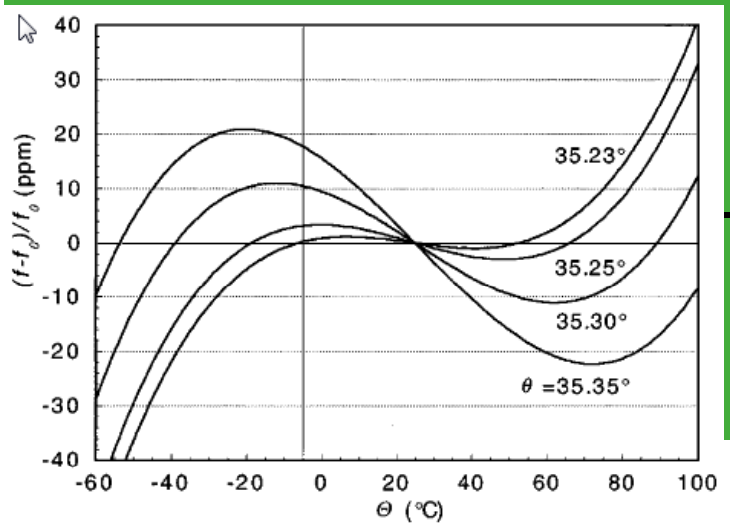
Yong, Y.-K., Patel, M.S., Tanaka, M.: Effects of thermal stresses on the frequency–temperature behavior of piezoelectric resonators. *J. Therm. Stress*, 30, 639–661, 2007. DOI:10.1080/01495730701274252

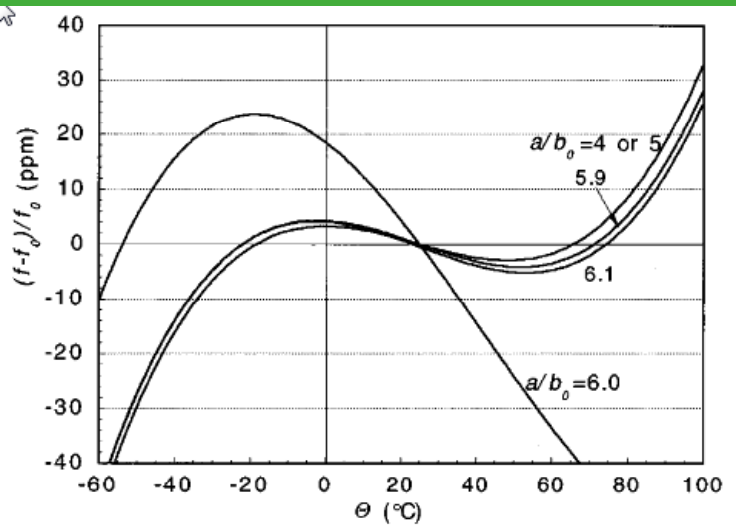
Drive Level Dependence

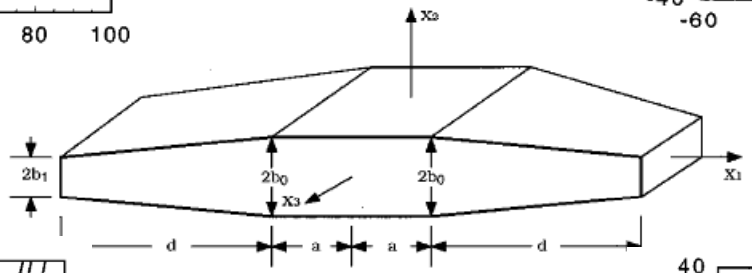
Another phenomenon of resonator malfunctioning is the drive-level dependence (DLD), which shows the frequency and property variation with the increase of driving voltage in the circuit. Clearly, this is one of the vital properties in many critical applications because the service can be fatally disrupted. Later investigations have been shown that the DLD is closely related to the nonlinear properties of quartz crystal and the nonlinear vibrations of plates. The resonator properties are different under the influence of strong electrical field. Such an analysis and prediction are presented with the finite element analysis with the consideration of nonlinear vibrations of piezoelectric plates.

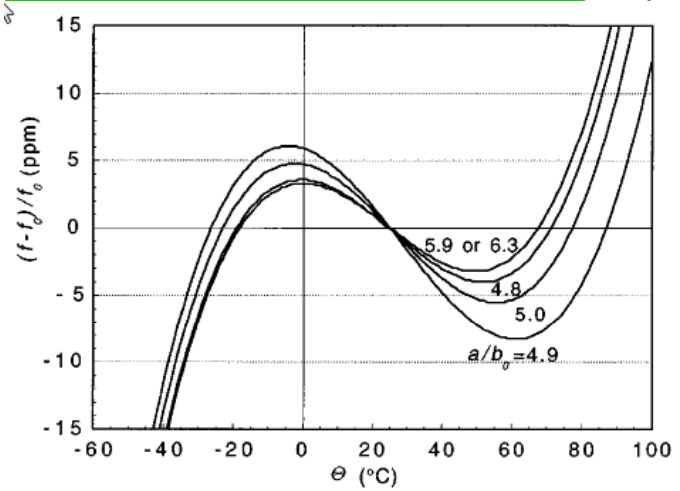
Mihir S Patel, Yook-Kong Yong, and Masako Tanaka, Drive level dependency in quartz resonators, *Intl. J. of Solids Struct.*, **46** (9), 1856-1871, 2009. doi:10.1016/j.ijsolstr.2008.12.021

Beveling

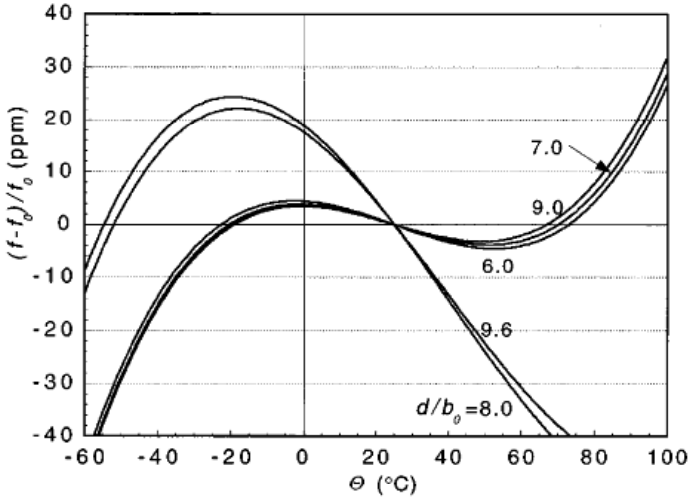








P. C. Y. Lee and J. Wang, Frequency–temperature relations of thickness-shear and flexural vibrations of contoured quartz resonators, *J. Appl. Phys.* **80** (6), 3457-3465,1996.



致谢

国家自然科学基金委员会
National Natural Science Foundation of China

中华人民共和国教育部
Ministry of Education of the People's Republic of China

浙江省科学技术厅
Science and Technology Department of Zhejiang Province

TXC 台晶(寧波)電子
TXC (NINGBO) Corp.

2012全国压电会议

2012年全国压电与声波理论及器件技术研讨会

Spawda 2012

上海交通大学

2012年11月21-24日

会议网站

http://spawda2012.sjtu.edu.cn

谢谢大家参加！

请将您的建议和问题发到

wangji@nbu.edu.cn

宁波大学压电器件技术实验室的更多信息

http://piezo.nbu.edu.cn

基于Mindlin板理论的石英晶体谐振器高频振动分析



王骥 教授
宁波大学压电器件技术实验室
http://piezo.nbu.edu.cn
wangji@nbu.edu.cn

2012压电声波器件分析理论与方法暑期讲习班
2012年8月6-9日·宁波大学